J. Shanghai Jiaotong Univ. (Sci.), 2015, 20(5): 513-527
DOI: 10.1007/s12204-015-1659-y

H_∞ Inverse Optimal Adaptive Fault-Tolerant Attitude Control for Flexible Spacecraft with Input Saturation

LONG Hai-hui (龙海辉), *ZHAO Jian-kang** (赵健康), *LAI Jian-qing* (赖剑清)
(Shanghai Key Laboratory of Navigation and Location Based Services, Shanghai Jiaotong University, Shanghai 200240, China)

Abstract: An adaptive inverse optimal attitude controller for flexible spacecraft with fault-free actuator is designed based on adaptive control Lyapunov function and inverse optimal methodology subjected to unknown parameter uncertainties, external disturbances and input saturation. The partial loss of actuator effectiveness and the additive faults are considered simultaneously to deal with actuator faults, and the prior knowledge of bounds on the effectiveness factors of the actuators is assumed to be unknown. A fault-tolerant control version is designed to handle the system with actuator fault by introducing a parameter update law to estimate the lower bound of the partial loss of actuator effectiveness faults. The proposed fault-tolerant attitude controller ensures robustness and stabilization, and it achieves H_∞ optimality with respect to a family of cost functionals. The usefulness of the proposed algorithms is assessed and compared with the conventional approaches through numerical simulations.
Key words: fault-tolerant, attitude control, inverse optimization, flexible spacecraft, adaptive control, input saturation
CLC number: TP 13 **Document code:** A

0 Introduction

Stability and accuracy are of prime importance in the satellite attitude control. However, during the spacecraft mission, factors like aging and accident may cause damage to the actuators and sensors. Actuator faults can lead to control system instability or even end up with catastrophic events if they are not well handled. Hence, fault tolerance of the spacecraft attitude control system is one of the crucial issues that need to be studied. Fault-tolerant control (FTC) has been counted as one of the most promising control technologies for maintaining the specified safety performance of a system in the presence of unexpected faults. Several FTC methods have been proposed for attitude control of a spacecraft in recent years[1-5]. Xiao and Hu[6] addressed a fault-tolerant controller for a flexible spacecraft to effectively accommodate the case where both the loss of control effectiveness and the additive faults occurred in actuators simultaneously. However, in that paper the knowledge of the lower bound of the effectiveness factor was needed to implement the controller. In addition, control input saturation in the controller design was not considered explicitly. In fact, due to the physical limitations in practice, the outputs of the actuator are constrained. As an actuator reaches its input limit, any effort to further increase the actuator output would result in no variation in the output, which may lead to a performance deterioration or even instability of the system[4]. Hence taking control input saturation explicitly into account in the attitude control algorithm is of interest and significance in practice[7-8]. Although control input saturation and fault tolerance were considered by Cai et al.[9] and Zou and Kumar[10] in the control design, the information about the lower bound of the effectiveness factor was needed, and the additive fault was not taken into account. Hu and Xiao[11] proposed a fault-tolerant sliding mode attitude controller for a spacecraft with input saturation, and the knowledge of the lower bound of the effectiveness factor was not needed via the adaptive estimate method. However, the degree of optimality of that controller was not presented explicitly, and once again the additive fault was not considered.

It is well known in optimal control theory that the optimal feedback systems enjoy several desirable stability and robustness properties as long as the optimization is meaningful[12]. An additional consequence of

Received date: 2013-11-20
Foundation item: the National High Technology Research and Development Program (863) of China (No. 2012AA121602) and the Preliminary Research Program of the General Armament Department of China (No. 51322050202)
***E-mail:** zhaojiankang@sjtu.edu.cn

optimality is the fact that the robust optimal controllers do not waste unnecessary control effort to achieve robust stabilization. Therefore, optimality is a key prerequisite for any controller design strategy that tries to effectively address the problem. Furthermore, the benefits of optimality listed above do not depend on the specific choice of the performance index as long as it is a meaningful one. In recent years, increasing attention has been focused on the optimal control problems of a spacecraft[13-18]. Even though the above works provide the controllers that are optimal with respect to a meaningful cost, in general, they do not lead to accurate and reliable attitude control when the faults or disturbances occur in the components, actuators and sensors. Recently, the H_∞ optimal fault-tolerant control[19] was addressed for a rigid satellite with time-varied actuator fault. Though fault-tolerant was considered and robust optimality was achieved in that control design, the associated Hamilton-Jacobi-Isaacs partial differential (HJIPD) equation solution was a big challenge due to the high nonlinearity of the attitude dynamics model. Therefore, the practical application of that method was still questionable.

A so-called inverse optimal control[20-22] is an alternative method to solve the nonlinear optimal control problem by circumventing the need to solve the HJIPD equation directly. The method was first addressed by Bharadwaj et al.[23] and Krstić and Tsiotras[24] to solve the attitude control problem. They designed an inverse optimal feedback controller for the attitude regulation problem of a rigid spacecraft without external disturbances and uncertainties in the inertia matrix. Later, the H_∞ inverse optimal attitude-tracking controller with respect to extended disturbances[25] and the adaptive inverse optimal control with external disturbance and uncertainty inertial matrix for a rigid spacecraft[26] were proposed. In Ref. [26], an adaptive control Lyapunov function was employed to deal with the uncertainty of the inertial matrix. However, these proposed inverse optimal approaches were limited only to dealing with rigid spacecraft and thereby could hardly directly be extended to the flexible spacecraft system, since the vibration in the flexible appendages induced by the orbiting attitude slewing operation may degrade the attitude pointing accuracy. Moreover, these controllers did not explicitly consider actuator faults and input saturation, and so could not be applied directly to the spacecraft system with actuator faults and control constraint.

In this work, a novel fault-tolerant attitude control strategy is addressed for flexible spacecraft to overcome the shortcomings of the preceding research for the spacecraft attitude control systems. The saturation compensator based on radial basis function (RBF) neural network (NN) is employed to reduce the effect of the control input saturation of system. The additive faults and the partial loss of actuator effectiveness are considered simultaneously in the attitude controller design, and the lower bound of the actuator effectiveness factor is assumed to be unknown. Three adaptive parameter update laws are addressed to estimate the weight matrix of neural network, the lower bound of the partial loss actuator effectiveness factor and the unknown inertia matrix, respectively. The attitude of spacecraft is represented by the unit quaternion, which is singularity-free. The proposed fault-tolerant attitude controller accounting for control input saturation is explicitly optimal with respect to a family of cost functionals and achieves the H_∞ disturbance attenuation without solving the associated HJIPD equation directly subjected to the actuator failures, uncertainty inertia matrix and external disturbances. The derived control law can achieve the goal of fault-tolerant control without the need of any fault detection and isolation mechanism to determine the fault information.

1 Model Description and Problem Formulation

This section briefly introduces the attitude motion of a flexible spacecraft with actuator faults, which incorporates the attitude kinematics and spacecraft dynamic equations.

A unit quaternion is employed to represent the attitude of the spacecraft, which is free of singularity. The unit quaternion $\boldsymbol{Q}$ is defined by

$$\boldsymbol{Q} = \begin{bmatrix} q_0 \\ \boldsymbol{q} \end{bmatrix} = \begin{bmatrix} \cos(\theta/2) \\ \boldsymbol{e}\sin(\theta/2) \end{bmatrix}, \tag{1}$$

where, $\boldsymbol{e} \in \mathbf{R}^3$ and θ denote the Euler axis and Euler angle, respectively; $\boldsymbol{q} = [q_1 \;\; q_2 \;\; q_3]^{\mathrm{T}} \in \mathbf{R}^3$ and $q_0 \in \mathbf{R}^1$ are called the vector part and the scalar part of the unit quaternion, respectively. The quaternion $\boldsymbol{Q}$ satisfies the unit norm constraint $\|\boldsymbol{Q}\| = 1$. Then, the kinematic equation is given by

$$\dot{\boldsymbol{Q}} = \begin{bmatrix} \dot{q}_0 \\ \dot{\boldsymbol{q}} \end{bmatrix} = \frac{1}{2}\begin{bmatrix} -\boldsymbol{q}^{\mathrm{T}} \\ \boldsymbol{q}^{\times} + q_0\boldsymbol{I}_3 \end{bmatrix}\boldsymbol{\omega}, \tag{2}$$

where $\boldsymbol{\omega} \in \mathbf{R}^3$ is the angular velocity of the spacecraft with respect to an inertial frame $\mathcal{I}$ and expressed in the body frame $\mathcal{B}$, $\boldsymbol{I}_3 \in \mathbf{R}^{3\times 3}$ is the identity matrix, and symbol "$\times$" is an operator on the three-dimensional vector $\boldsymbol{q}$ such that $\boldsymbol{q}^{\times}$ denotes

$$\boldsymbol{q}^{\times} = \begin{bmatrix} 0 & -q_3 & q_2 \\ q_3 & 0 & -q_1 \\ -q_2 & q_1 & 0 \end{bmatrix}, \tag{3}$$

which is a skew-symmetric matrix.

Next, consider the dynamic equations of a flexible spacecraft. Here, both the partial loss of control effective and the additive faults in actuators are considered simultaneously, and the general nonlinear spacecraft attitude dynamic model can be given by[6]

$$\begin{aligned}&\boldsymbol{J}_\mathrm{s}\dot{\boldsymbol{\omega}}+\boldsymbol{\sigma}^\mathrm{T}\ddot{\boldsymbol{\eta}}=\\&\qquad-\boldsymbol{\omega}\times(\boldsymbol{J}_\mathrm{s}\boldsymbol{\omega}+\boldsymbol{\sigma}^\mathrm{T}\dot{\boldsymbol{\eta}})+(\boldsymbol{\delta u}+\boldsymbol{f})+\boldsymbol{d}_\mathrm{s},\end{aligned}\tag{4}$$

$$\ddot{\boldsymbol{\eta}}+\boldsymbol{D}\dot{\boldsymbol{\eta}}+\boldsymbol{E}\boldsymbol{\eta}+\boldsymbol{\sigma}\dot{\boldsymbol{\omega}}=\boldsymbol{0},\tag{5}$$

where, $\boldsymbol{J}_\mathrm{s}\in\mathbf{R}^{3\times3}$ is the symmetric inertia matrix of the whole structure; $\boldsymbol{\eta}\in\mathbf{R}^N$ is the model coordinate vector; $\boldsymbol{\sigma}\in\mathbf{R}^{N\times3}$ is the coupling matrix between the elastic and rigid structures; $\boldsymbol{u}\in\mathbf{R}^3$ is the actual control torques generated by the actuators or thrusters; $\boldsymbol{d}_\mathrm{s}\in\mathbf{R}^3$ is a term taking disturbance torque into account; whereas, $\boldsymbol{D}=\mathrm{diag}\{2\xi_i\Lambda_i^{1/2},\ i=1,2,\cdots,N\}$ and $\boldsymbol{E}=\mathrm{diag}\{\Lambda_i, i=1,2,\cdots,N\}$ are the damping and stiffness matrices, respectively, in which N is the number of elastic modes considered, ξ_i is the corresponding damping ratio, and $\Lambda_i^{1/2}$ is the natural frequency; $\boldsymbol{\delta}=\mathrm{diag}\{\delta_{11},\delta_{22},\delta_{33}\}$ denotes the partial loss of actuator effectiveness fault with

$$0<\mu\leqslant\delta_{ii}\leqslant1,\quad i=1,2,3,\tag{6}$$

and $\boldsymbol{f}\in\mathbf{R}^3$ represents the additive actuator fault.

Remark 1 Note that, if $\boldsymbol{\delta}=\boldsymbol{I}_3$ and $\boldsymbol{f}=\boldsymbol{0}_{3\times1}$ in the attitude control of the whole process, then the dynamic system in Eqs. (4) and (5) becomes the nominal system in which all of the actuators are fault-free[6].

Remark 2 In fact, due to onboard payload motion, rotation of solar arrays, fuel consumption and out-gassing during operation, the inertial matrix $\boldsymbol{J}_\mathrm{s}$ of spacecraft may be time varying. Here, we divide it into two parts, i.e., $\boldsymbol{J}_\mathrm{s}=\boldsymbol{J}+\Delta\boldsymbol{J}$, where $\boldsymbol{J}$ and $\Delta\boldsymbol{J}$ represent the nominal value component and the parameter perturbation component of the inertial matrix $\boldsymbol{J}_\mathrm{s}$, respectively. Both of the nominal value component of $\boldsymbol{J}$ and the perturbation matrix $\Delta\boldsymbol{J}$ are symmetric since $\boldsymbol{J}_\mathrm{s}$ is always a symmetric matrix.

If the terms $\Delta\boldsymbol{J}\dot{\boldsymbol{\omega}}$ and $\boldsymbol{\omega}\times\Delta\boldsymbol{J}\boldsymbol{\omega}$ are considered as the disturbances, then Eq. (4) can be rewritten as

$$\boldsymbol{J}\dot{\boldsymbol{\omega}}+\boldsymbol{\sigma}^\mathrm{T}\ddot{\boldsymbol{\eta}}=-\boldsymbol{\omega}\times(\boldsymbol{J}\boldsymbol{\omega}+\boldsymbol{\sigma}^\mathrm{T}\dot{\boldsymbol{\eta}})+\boldsymbol{\delta u}+(\boldsymbol{d}+\boldsymbol{f}),\tag{7}$$

where $\boldsymbol{d}(t)=\Delta\boldsymbol{J}\dot{\boldsymbol{\omega}}-\boldsymbol{\omega}\times\Delta\boldsymbol{J}\boldsymbol{\omega}+\boldsymbol{d}_\mathrm{s}(t)$ is considered as the lumped disturbance of spacecraft.

Throughout this paper, the following assumptions are considered.

Assumption 1 The nominal components $\boldsymbol{J}$ and $(\boldsymbol{J}-\boldsymbol{\sigma}^\mathrm{T}\boldsymbol{\sigma})$ are unknown positive definite symmetric and bounded constant matrices.

Assumption 2 The lumped disturbance $\boldsymbol{d}$ and the extended disturbance $(\boldsymbol{d}+\boldsymbol{f})$ in the flexible spacecraft system Eq. (7) are unknown but bounded with a known bound, i.e., $\displaystyle\int_0^t\|\boldsymbol{d}(\kappa)\|^2\mathrm{d}\kappa<\infty$ and $\displaystyle\int_0^t\|\boldsymbol{d}(\kappa)+\boldsymbol{f}(\kappa)\|^2\mathrm{d}\kappa<\infty$ for all finite $t\geqslant0$, where $\|\cdot\|$ denotes the Euclidean norm.

Assumption 3 The lower bound μ of the partial loss of actuator effectiveness faults is unknown.

Assumption 4 The actual control torque $\boldsymbol{u}(t)=[u_1(t)\ \ u_2(t)\ \ u_3(t)]^\mathrm{T}$ is constrained, that is

$$\|\boldsymbol{u}\|\leqslant\tau_{\max},\tag{8}$$

where $\tau_{\max}>0$ is a known constant.

In this paper, we consider the rest-to-test maneuvers. For the fault attitude system consists of Eqs. (2), (4) and (5), under Assumptions 1—4, the control objective is to design a fault-tolerant controller to realize the desired rotations and, at the same time, to damp out the vibrations induced by these maneuvers in the flexible elements of the spacecraft and in the presence of actuator faults, control input saturation, uncertainty inertia matrix and external disturbances. The problem at hand can be summarized as follows. Find a controller $\boldsymbol{u}$ subjected to Eq. (8) such that for all physically realizable initial conditions, the desired rotations are achieved, i.e.,

$$\lim_{t\to\infty}\boldsymbol{q}=\boldsymbol{0},\quad\lim_{t\to\infty}q_0=1,\quad\lim_{t\to\infty}\boldsymbol{\omega}=\boldsymbol{0},\tag{9}$$

and at the same time, the vibrations induced by the maneuver rotation are also damped out, i.e.,

$$\lim_{t\to\infty}\boldsymbol{\eta}=\boldsymbol{0},\quad\lim_{t\to\infty}\dot{\boldsymbol{\eta}}=\boldsymbol{0}.\tag{10}$$

It is worth noting that when $\boldsymbol{q}\to\boldsymbol{0}$, we have $q_0\to1$ due to the constraint relation.

2 Inverse Optimal Control for Flexible Spacecraft

2.1 Mathematical Preliminaries

Consider the nonlinear dynamic system

$$\dot{\boldsymbol{x}}=\boldsymbol{f}(\boldsymbol{x})+\boldsymbol{F}(\boldsymbol{x})\boldsymbol{\theta}+\boldsymbol{g}_1(\boldsymbol{x})\boldsymbol{d}+\boldsymbol{g}_2(\boldsymbol{x})\boldsymbol{u},\tag{11}$$

where $\boldsymbol{x}\in\mathbf{R}^n$ is the state, $\boldsymbol{u}\in\mathbf{R}^p$ is the input, $\boldsymbol{d}\in\mathbf{R}^s$ is the disturbance, $\boldsymbol{f}:\mathbf{R}^n\to\mathbf{R}^n$, $\boldsymbol{F}:\mathbf{R}^n\to\mathbf{R}^{n\times m}$, $\boldsymbol{g}_1:\mathbf{R}^n\to\mathbf{R}^{n\times s}$ and $\boldsymbol{g}_2:\mathbf{R}^n\to\mathbf{R}^{n\times p}$ are the smooth vector- or matrix-valued functions, respectively, and $\boldsymbol{\theta}\in\mathbf{R}^m$ is a constant unknown parameter vector. Besides, $\hat{\boldsymbol{\theta}}$ denotes an estimate of $\boldsymbol{\theta}$ with the estimation error $\tilde{\boldsymbol{\theta}}=\boldsymbol{\theta}-\hat{\boldsymbol{\theta}}$ and $\|\tilde{\boldsymbol{\theta}}\|^2_{\boldsymbol{\Gamma}^{-1}}=\tilde{\boldsymbol{\theta}}^\mathrm{T}\boldsymbol{\Gamma}^{-1}\tilde{\boldsymbol{\theta}}$.

Definition 1[27] A smooth function $V(\boldsymbol{x},\boldsymbol{\theta})$: $\mathbf{R}^n\times\mathbf{R}^n\to\mathbf{R}_\perp$, positive definite and radially unbounded in $\boldsymbol{x}$ for each $\boldsymbol{\theta}$, is called an adaptive control Lyapunov function (ACLF) for the nonlinear dynamic system

$$\dot{\boldsymbol{x}}=\boldsymbol{f}(\boldsymbol{x})+\boldsymbol{F}(\boldsymbol{x})\boldsymbol{\theta}+\boldsymbol{g}_2(\boldsymbol{x})\boldsymbol{u}.\tag{12}$$

There exist a positive definite symmetric matrix $\boldsymbol{\Gamma} \in \mathbf{R}^{p\times p}$, a continuous function $\boldsymbol{W}(\boldsymbol{x},\boldsymbol{\theta})$ positive definite in $\boldsymbol{x}$ for each $\boldsymbol{\theta} \in \mathbf{R}^p$ and a control $\boldsymbol{u} = \boldsymbol{\alpha}(\boldsymbol{x},\boldsymbol{\theta})$ smooth on $(\mathbf{R}^n\backslash\{0\}) \times \mathbf{R}^p$ with $\boldsymbol{\alpha}(\mathbf{0},\boldsymbol{\theta}) \equiv \mathbf{0}$ such that $V(\boldsymbol{x},\boldsymbol{\theta})$ satisfies

$$\frac{\partial V}{\partial \boldsymbol{x}}\left\{\boldsymbol{f} + \boldsymbol{F}\left[\boldsymbol{\theta} + \boldsymbol{\Gamma}\left(\frac{\partial V}{\partial \boldsymbol{\theta}}\right)\right]^{\mathrm{T}} + \boldsymbol{g}_2\boldsymbol{u}\right\} \leqslant -\boldsymbol{W}(\boldsymbol{x},\boldsymbol{\theta}), \tag{13}$$

for the auxiliary system

$$\dot{\boldsymbol{x}} = \boldsymbol{f}(\boldsymbol{x}) + \boldsymbol{F}(\boldsymbol{x})\left[\boldsymbol{\theta} + \boldsymbol{\Gamma}\left(\frac{\partial V}{\partial \boldsymbol{\theta}}\right)^{\mathrm{T}}\right] + \boldsymbol{g}_2(\boldsymbol{x})\boldsymbol{u}. \tag{14}$$

Definition 2[26] Consider the nonlinear system in Eq. (11) and the auxiliary system

$$\dot{\boldsymbol{x}} = \boldsymbol{f}(\boldsymbol{x}) + \boldsymbol{F}(\boldsymbol{x})\left[\boldsymbol{\theta} + \boldsymbol{\Gamma}\left(\frac{\partial V}{\partial \boldsymbol{\theta}}\right)^{\mathrm{T}}\right] + \frac{1}{\gamma^2}\boldsymbol{g}_1(\boldsymbol{x})(L_{\boldsymbol{g}_1}V)^{\mathrm{T}} + \boldsymbol{g}_2(\boldsymbol{x})\boldsymbol{u}, \tag{15}$$

where $\gamma > 0$, $V(\boldsymbol{x},\boldsymbol{\theta})$ is a Lyapunov function candidate, $L_{\boldsymbol{g}_1}V$ denotes the Lie derivative of the Lyapunov function $V(\boldsymbol{x})$ with respect to $\boldsymbol{g}_1(\boldsymbol{x})$, i.e., $L_{\boldsymbol{g}_1}V = [\partial V(\boldsymbol{x})/\partial \boldsymbol{x}]\boldsymbol{g}_1(\boldsymbol{x})$. Suppose that there exists a real matrix $\boldsymbol{R}_2(\boldsymbol{x},\boldsymbol{\theta}) = \boldsymbol{R}_2^{\mathrm{T}}(\boldsymbol{x},\boldsymbol{\theta}) > \mathbf{0}$ such that the control law

$$\boldsymbol{u} = \boldsymbol{\alpha}(\boldsymbol{x},\boldsymbol{\theta}) = -\boldsymbol{R}_2^{-1}(\boldsymbol{x},\boldsymbol{\theta})(L_{\boldsymbol{g}_2}V)^{\mathrm{T}} \tag{16}$$

asymptotically stabilizes Eq. (15) with respect to $V(\boldsymbol{x},\boldsymbol{\theta})$. Then, the dynamic feedback control

$$\boldsymbol{u} = \boldsymbol{\alpha}^*(\boldsymbol{x},\hat{\boldsymbol{\theta}}) = -2\boldsymbol{R}_2^{-1}(\boldsymbol{x},\hat{\boldsymbol{\theta}})(L_{\boldsymbol{g}_2}V)^{\mathrm{T}}, \tag{17}$$

$$\dot{\hat{\boldsymbol{\theta}}} = \boldsymbol{\Gamma}\boldsymbol{\tau}(\boldsymbol{x},\hat{\boldsymbol{\theta}}) = \boldsymbol{\Gamma}(L_{\boldsymbol{F}}V)^{\mathrm{T}} \tag{18}$$

can solve the H_∞ inverse optimal adaptive control problem for the nonlinear system Eq. (11) by minimizing the cost functional

$$J_a = \sup_{\boldsymbol{d}\in\mathcal{D}}\left\{\lim_{t\to\infty}\left[4V(\boldsymbol{x}(t),\hat{\boldsymbol{\theta}}(t)) + \int_0^t \left(l(\boldsymbol{x},\hat{\boldsymbol{\theta}}) + \boldsymbol{u}^{\mathrm{T}}\boldsymbol{R}_2(\boldsymbol{x},\hat{\boldsymbol{\theta}})\boldsymbol{u} - \gamma^2\|\boldsymbol{d}\|^2\right)\mathrm{d}\kappa\right]\right\}, \tag{19}$$

where

$$l(\boldsymbol{x},\hat{\boldsymbol{\theta}}) = -4L_{\boldsymbol{f}}V - 4L_{\boldsymbol{F}}V\left[\hat{\boldsymbol{\theta}} + \boldsymbol{\Gamma}\left(\frac{\partial V}{\partial \hat{\boldsymbol{\theta}}}\right)^{\mathrm{T}}\right] - \frac{4}{\gamma^2}L_{\boldsymbol{g}_1}V(L_{\boldsymbol{g}_1}V)^{\mathrm{T}} + 4L_{\boldsymbol{g}_2}V\boldsymbol{R}_2^{-1}(L_{\boldsymbol{g}_2}V)^{\mathrm{T}}, \tag{20}$$

$\mathcal{D}$ is the set of locally bounded functions of $\boldsymbol{x}$. Here, $l(\boldsymbol{x},\hat{\boldsymbol{\theta}})$ is positive definite in $\boldsymbol{x}$ for each $\hat{\boldsymbol{\theta}} \in \mathbf{R}^m$.

Remark 3 Definition 2 is a direct result of Theorem 3 and Definition 4 of Ref. [26]. As mentioned in Ref. [26], the H_∞ adaptive inverse optimal controller $\boldsymbol{u} = \boldsymbol{\alpha}^*(\boldsymbol{x},\hat{\boldsymbol{\theta}})$ in Eq. (10) achieves γ-level of the H_∞ disturbance attenuation for all $t \geqslant 0$ and for each $\boldsymbol{\theta} \in \mathbf{R}^m$. Compared with the nonlinear H_∞ control, the inverse optimal method solves the nonlinear optimal-assignment problem with respect to a meaningful cost functional without solving the HJIPD equation explicitly.

2.2 H_∞ Inverse Optimal Adaptive Fault-Tolerant Attitude Control for Flexible Spacecraft with Actuator Faults

Note that kinematic equation given by Eq. (2) describes a system in cascade interconnection, which implies that the system is controlled indirectly through the angular velocity vector $\boldsymbol{\omega}$. Therefore, $\boldsymbol{\omega}$ can be regarded as the virtual control input to stabilize the kinematic system, and the control law can be designed as follows:

$$\boldsymbol{\omega}_{\mathrm{d}} = -\boldsymbol{K}\boldsymbol{q}, \tag{21}$$

with $\boldsymbol{K} \in \mathbf{R}^{3\times 3}$ and $\boldsymbol{K} = \boldsymbol{K}^{\mathrm{T}} > \mathbf{0}$. It has been proved in Ref. [16] that the control law $\boldsymbol{\omega}_{\mathrm{d}}$ globally asymptotically stabilizes the kinematic system at the origin.

For the simplicity of the development, the total angular velocity expressed in model variables is introduced as follows:

$$\boldsymbol{\nu} = \boldsymbol{\sigma}\boldsymbol{\omega} + \dot{\boldsymbol{\eta}}. \tag{22}$$

Note that

$$\dot{\boldsymbol{\nu}} = \boldsymbol{\sigma}\dot{\boldsymbol{\omega}} + \ddot{\boldsymbol{\eta}} = -\boldsymbol{D}\boldsymbol{\nu} - \boldsymbol{E}\boldsymbol{\eta} + \boldsymbol{D}\boldsymbol{\sigma}\boldsymbol{\omega}.$$

Therefore, given

$$\boldsymbol{\xi} = [\boldsymbol{\eta}^{\mathrm{T}} \quad \boldsymbol{\nu}^{\mathrm{T}}]^{\mathrm{T}} \tag{23}$$

and according to Eq. (5), the following equation can be yielded as

$$\dot{\boldsymbol{\xi}} = \boldsymbol{A}\boldsymbol{\xi} + \boldsymbol{B}\boldsymbol{\omega}, \tag{24}$$

where

$$\boldsymbol{A} = \begin{bmatrix} \mathbf{0} & \boldsymbol{I} \\ -\boldsymbol{E} & -\boldsymbol{D} \end{bmatrix}, \quad \boldsymbol{B} = \begin{bmatrix} -\boldsymbol{\sigma} \\ \boldsymbol{D}\boldsymbol{\sigma} \end{bmatrix}, \tag{25}$$

$\boldsymbol{I} \in \mathbf{R}^{N\times N}$ is the identity matrix.

In view of Eqs. (7) and (24), one has

$$(\boldsymbol{J} - \boldsymbol{\sigma}^{\mathrm{T}}\boldsymbol{\sigma})\dot{\boldsymbol{\omega}} = -\boldsymbol{\omega}^\times\boldsymbol{J}\boldsymbol{\omega} + [\boldsymbol{\sigma}^{\mathrm{T}}\boldsymbol{E} \quad \boldsymbol{\sigma}^{\mathrm{T}}\boldsymbol{D} - \boldsymbol{\omega}^\times\boldsymbol{\sigma}^{\mathrm{T}}]\boldsymbol{\xi} - (\boldsymbol{\sigma}^{\mathrm{T}}\boldsymbol{D} - \boldsymbol{\omega}^\times\boldsymbol{\sigma}^{\mathrm{T}})\boldsymbol{\sigma}\boldsymbol{\omega} + \boldsymbol{\delta}\boldsymbol{u} + \boldsymbol{d} + \boldsymbol{f}. \tag{26}$$

To isolate the inertia parameters $J_{ij}(i,j = 1,2,3)$, we define a linear operator $\boldsymbol{L} : \mathbf{R}^3 \to \mathbf{R}^{3\times 6}$ acting on $\boldsymbol{b} = [b_1 \quad b_2 \quad b_3]^{\mathrm{T}}$ by[28]

$$\boldsymbol{L}(\boldsymbol{b}) = \begin{bmatrix} b_1 & 0 & 0 & 0 & b_3 & b_2 \\ 0 & b_2 & 0 & b_3 & 0 & b_1 \\ 0 & 0 & b_3 & b_2 & b_1 & 0 \end{bmatrix}.$$

Let $\boldsymbol{\vartheta} = [J_{11} \quad J_{22} \quad J_{33} \quad J_{23} \quad J_{13} \quad J_{12}]$. Then $\boldsymbol{Jb} = \boldsymbol{L}(\boldsymbol{b})\boldsymbol{\vartheta}$. Let $\hat{\boldsymbol{\vartheta}} = [\hat{J}_{11} \quad \hat{J}_{22} \quad \hat{J}_{33} \quad \hat{J}_{23} \quad \hat{J}_{13} \quad \hat{J}_{12}]$ represent the parameter estimate of $\boldsymbol{\vartheta}$. The estimation error $\tilde{\boldsymbol{\vartheta}}$ is defined by $\tilde{\boldsymbol{\vartheta}} = \boldsymbol{\vartheta} - \hat{\boldsymbol{\vartheta}}$. Define the expected error as follows:

$$\boldsymbol{x} = \boldsymbol{\omega} - \boldsymbol{\omega}_{\mathrm{d}} = \boldsymbol{\omega} + \boldsymbol{K}\boldsymbol{q}. \tag{27}$$

As a result, the subsystem Eq. (26) becomes

$$\begin{aligned}\boldsymbol{J}_\sigma \dot{\boldsymbol{x}} = &[\boldsymbol{\phi}(\boldsymbol{\omega}) + \boldsymbol{\varphi}(\boldsymbol{q}, q_0, \boldsymbol{\omega})]\boldsymbol{\vartheta} + \boldsymbol{r}_1(\boldsymbol{\omega})\boldsymbol{\xi} + \\ &\boldsymbol{r}_2(\boldsymbol{q}, q_0, \boldsymbol{\omega})\boldsymbol{\omega} + \boldsymbol{\delta u} + \boldsymbol{d} + \boldsymbol{f},\end{aligned} \tag{28}$$

where $\boldsymbol{J}_\sigma \in \mathbf{R}^{3\times3}$, $\boldsymbol{\phi}(\boldsymbol{\omega}) \in \mathbf{R}^{3\times6}$, $\boldsymbol{\varphi}(\boldsymbol{q}, q_0, \boldsymbol{\omega}) \in \mathbf{R}^{3\times6}$, $\boldsymbol{r}_1(\boldsymbol{\omega}) \in \mathbf{R}^{3\times1}$ and $\boldsymbol{r}_2(\boldsymbol{q}, q_0, \boldsymbol{\omega}) \in \mathbf{R}^{3\times1}$ are expressed by

$$\boldsymbol{J}_\sigma = \boldsymbol{J} - \boldsymbol{\sigma}^{\mathrm{T}}\boldsymbol{\sigma}, \tag{29}$$

$$\boldsymbol{\phi}(\boldsymbol{\omega}) = -\boldsymbol{\omega}^\times \boldsymbol{L}(\boldsymbol{\omega}), \tag{30}$$

$$\boldsymbol{\varphi}(\boldsymbol{q}, q_0, \boldsymbol{\omega}) = \boldsymbol{L}\Big(\frac{1}{2}\boldsymbol{K}(q_0\boldsymbol{I}_3 + \boldsymbol{q}^\times)\boldsymbol{\omega}\Big), \tag{31}$$

$$\boldsymbol{r}_1(\boldsymbol{\omega}) = [\boldsymbol{\sigma}^{\mathrm{T}}\boldsymbol{E} \quad \boldsymbol{\sigma}^{\mathrm{T}}\boldsymbol{D} - \boldsymbol{\omega}^\times\boldsymbol{\sigma}^{\mathrm{T}}], \tag{32}$$

$$\begin{aligned}\boldsymbol{r}_2(\boldsymbol{q}, q_0, \boldsymbol{\omega}) = &-(\boldsymbol{\sigma}^{\mathrm{T}}\boldsymbol{D} - \boldsymbol{\omega}^\times\boldsymbol{\sigma}^{\mathrm{T}})\boldsymbol{\sigma} - \\ &\frac{1}{2}\boldsymbol{\sigma}^{\mathrm{T}}\boldsymbol{\sigma}\boldsymbol{K}(q_0\boldsymbol{I}_3 + \boldsymbol{q}^\times).\end{aligned} \tag{33}$$

Remark 4 It has been proven in Ref. [29] that for the kinematic subsystem in Eq. (2), $\lim\limits_{t\to\infty}\boldsymbol{q}(t) = \mathbf{0}$ can be achieved if there exists a control law $\boldsymbol{u}$ for Eq. (28) satisfying $\lim\limits_{t\to\infty}\boldsymbol{x}(t) = \mathbf{0}$ with any initial state, which implies that $\lim\limits_{t\to0}\boldsymbol{\omega}(t) = \mathbf{0}$ according to Eq. (27). Therefore, the achievement of $\lim\limits_{t\to\infty}\boldsymbol{q}(t) = \mathbf{0}$ and $\lim\limits_{t\to0}\boldsymbol{\omega}(t) = \mathbf{0}$ can be accomplished simultaneously only by $\lim\limits_{t\to\infty}\boldsymbol{x}(t) = \mathbf{0}$. Also from Eqs. (22) and (23), $\lim\limits_{t\to\infty}\boldsymbol{\eta}(t) = \mathbf{0}$ and $\lim\limits_{t\to\infty}\dot{\boldsymbol{\eta}}(t) = \mathbf{0}$ can be achieved if $\lim\limits_{t\to\infty}\boldsymbol{\xi} = \mathbf{0}$ and $\lim\limits_{t\to0}\boldsymbol{\omega}(t) = \mathbf{0}$ hold. Therefore, the achievement of $\lim\limits_{t\to\infty}\boldsymbol{q}(t) = \mathbf{0}$, $\lim\limits_{t\to0}\boldsymbol{\omega}(t) = \mathbf{0}$, $\lim\limits_{t\to\infty}\boldsymbol{\eta}(t) = \mathbf{0}$ and $\lim\limits_{t\to\infty}\dot{\boldsymbol{\eta}}(t) = \mathbf{0}$ can be accomplished simultaneously by $\lim\limits_{t\to\infty}\boldsymbol{x}(t) = \mathbf{0}$ and $\lim\limits_{t\to\infty}\boldsymbol{\xi} = \mathbf{0}$.

If the state vector is defined as $\boldsymbol{z} = [1 - q_0 \quad \boldsymbol{q} \quad \boldsymbol{x} \quad \boldsymbol{\xi}]^{\mathrm{T}}$, then the state-space representation of attitude control system in Eqs. (2), (4) and (8) can be obtained as

$$\dot{\boldsymbol{z}} = \boldsymbol{f}_1(\boldsymbol{z}) + \boldsymbol{f}_2(\boldsymbol{z})\boldsymbol{\vartheta} + \boldsymbol{h}_1(\boldsymbol{z})(\boldsymbol{d} + \boldsymbol{f}) + \boldsymbol{h}_2(\boldsymbol{z})\boldsymbol{u}, \tag{34}$$

where

$$\boldsymbol{f}_1(\boldsymbol{z}) = \begin{bmatrix} \frac{1}{2}\boldsymbol{q}\boldsymbol{\omega} \\ (\boldsymbol{q}^\times + q_0\boldsymbol{I}_3)\boldsymbol{\omega} \\ \boldsymbol{r}_1(\boldsymbol{\omega})\boldsymbol{\xi} + \boldsymbol{r}_2(\boldsymbol{q}, q_0, \boldsymbol{\omega})\boldsymbol{\omega} \\ \boldsymbol{A\xi} + \boldsymbol{B\omega} \end{bmatrix},$$

$$\boldsymbol{f}_2(\boldsymbol{z}) = \begin{bmatrix} \mathbf{0}_{1\times3} \\ \mathbf{0}_{3\times3} \\ \boldsymbol{\phi}(\boldsymbol{\omega}) + \boldsymbol{\varphi}(\boldsymbol{q}, q_0, \boldsymbol{\omega}) \\ \mathbf{0}_{2N\times3} \end{bmatrix},$$

$$\boldsymbol{h}_1(\boldsymbol{z}) = \begin{bmatrix} \mathbf{0}_{1\times3} \\ \mathbf{0}_{3\times3} \\ \boldsymbol{I}_3 \\ \mathbf{0}_{2N\times3} \end{bmatrix}, \quad \boldsymbol{h}_2(\boldsymbol{z}) = \begin{bmatrix} \mathbf{0}_{1\times3} \\ \mathbf{0}_{3\times3} \\ \boldsymbol{\delta} \\ \mathbf{0}_{2N\times3} \end{bmatrix}.$$

2.2.1 *Inverse Optimal Adaptive Controller (IOAC) Design for the Fault-Free System*

In this section, the H_∞ inverse optimal adaptive attitude controller is addressed using the adaptive control Lyapunov function and the inverse optimal approach in the case that the actuators are fault-free, i.e., $\boldsymbol{f} = \mathbf{0}_{3\times1}$ and $\boldsymbol{\delta} = \boldsymbol{I}_3$. Consider that $\boldsymbol{\vartheta}$ is an unknown constant vector. Therefore, an adaptive parameter update law is employed to estimate $\boldsymbol{\vartheta}$.

In practice, due to the physical constraints, the actuator saturation in the attitude control of spacecraft is unavoidable. The RBF NN based saturation compensator[30-31] is developed to compensate for the effects of input saturation on the system to guarantee that the resulting closed-loop attitude system is stable. Let

$$\boldsymbol{\ell}(\boldsymbol{x}) = \boldsymbol{u} - \boldsymbol{\tau}. \tag{35}$$

Here, $\boldsymbol{u} \in \mathbf{R}^3$ is the applied control torque acting on the spacecraft and $\boldsymbol{\tau} \in \mathbf{R}^3$ is the commanded control torque. According to the RBF NN approximation property[32], there exists an NN that is arbitrary closely approximated by $\boldsymbol{\ell}(\boldsymbol{x})$, that is

$$\boldsymbol{\ell}(\boldsymbol{x}) = \boldsymbol{\psi}^{\mathrm{T}}\boldsymbol{S}(\boldsymbol{x}) + \boldsymbol{\varepsilon}(\boldsymbol{x}), \tag{36}$$

where $\boldsymbol{S}(x) = [s_1(x) \quad s_2(x) \quad \cdots \quad s_m(\boldsymbol{x})] \in \mathbf{R}^m$ is a known continuous smooth vector-valued function, m is the NN node number, and $\boldsymbol{\varepsilon}(\boldsymbol{x})$ is the NN approximation error. The reconstruction error is bounded on a compact set $\boldsymbol{\Phi}$ by $\|\boldsymbol{\varepsilon}(\boldsymbol{x})\| \leqslant \varepsilon_{\mathrm{N}}$. Moreover, for any $\varepsilon_{\mathrm{N}} > 0$, one can find an NN such that $\|\boldsymbol{\varepsilon}(x)\| \leqslant \varepsilon_{\mathrm{N}}$ for all $\boldsymbol{x} \in \boldsymbol{\Phi}$; $\boldsymbol{\psi} \in \mathbf{R}^{3\times m}$ is the ideal target weight matrix. Specially, each argument $s_i(\boldsymbol{x})$ of $\boldsymbol{S}(\boldsymbol{x})$ is commonly chosen as Gaussian function $s_i(\boldsymbol{x}) = \exp(-|x_i - d_i|^2/a^2)$, where d_i is a constant called the center of $s_i(\boldsymbol{x})$ and $a > 0$ is a real number called the width of $s_i(\boldsymbol{x})$. Because the ideal target weight matrix $\boldsymbol{\psi}$ is difficult to determine, the implemented NN is actually an approximation of the ideal NN in Eq. (36) and is given by

$$\boldsymbol{\ell}(\boldsymbol{x}) = \hat{\boldsymbol{\psi}}^{\mathrm{T}}\boldsymbol{S}(\boldsymbol{x}), \tag{37}$$

where $\hat{\boldsymbol{\psi}}$ is the estimation of $\boldsymbol{\psi}$. Let $\hat{\boldsymbol{\ell}}$ be the estimation of $\boldsymbol{\ell}$. Let $\tilde{\boldsymbol{\ell}} = \boldsymbol{\ell} - \hat{\boldsymbol{\ell}}$ be the estimation error of $\boldsymbol{\ell}$ and $\tilde{\boldsymbol{\psi}} = \boldsymbol{\psi} - \hat{\boldsymbol{\psi}}$ be the estimation error of $\boldsymbol{\psi}$.

Theorem 1 Consider an auxiliary system that consists of Eqs. (2), (4) and the following equation

$$\boldsymbol{J_\sigma}\dot{\boldsymbol{x}} = (\boldsymbol{\phi}(\boldsymbol{\omega}) + \boldsymbol{\varphi}(\boldsymbol{q}, q_0, \boldsymbol{\omega}))\boldsymbol{\vartheta} + \boldsymbol{r}_1(\boldsymbol{\omega})\boldsymbol{\xi} + \boldsymbol{r}_2(\boldsymbol{q}, q_0, \boldsymbol{\omega})\boldsymbol{\omega} + \boldsymbol{u} + \frac{\boldsymbol{x}}{\gamma^2}, \tag{38}$$

for which Assumptions 1—4 hold, under the dynamic feedback control law

$$\boldsymbol{u} = \boldsymbol{\alpha}(\boldsymbol{q}, q_0, \boldsymbol{\omega}, \hat{\boldsymbol{\vartheta}}, \tau_{\max}) = -\boldsymbol{R}^{-1}(\boldsymbol{q}, q_0, \boldsymbol{\omega}, \hat{\boldsymbol{\vartheta}}, \tau_{\max})\boldsymbol{x} = \begin{cases} -\dfrac{\tau_{\max}\boldsymbol{x}}{2\|\boldsymbol{x}\|}, & \|\boldsymbol{\tau}\| > \dfrac{\tau_{\max}}{2} \\ \boldsymbol{\tau}, & \|\boldsymbol{\tau}\| \leqslant \dfrac{\tau_{\max}}{2} \end{cases} \tag{39}$$

together with the adaptive parameter update laws

$$\dot{\hat{\boldsymbol{\vartheta}}}(\boldsymbol{q}, q_0, \boldsymbol{\omega}) = \boldsymbol{\Pi}\boldsymbol{\pi}(\boldsymbol{q}, q_0, \boldsymbol{\omega}) = \boldsymbol{\Pi}[\boldsymbol{\phi}(\boldsymbol{\omega}) + \boldsymbol{\varphi}(\boldsymbol{q}, q_0, \boldsymbol{\omega})]^{\mathrm{T}}\boldsymbol{x}, \tag{40}$$

$$\dot{\hat{\boldsymbol{\psi}}} = \boldsymbol{\Gamma}\boldsymbol{S}(\boldsymbol{x})\boldsymbol{x}^{\mathrm{T}}, \tag{41}$$

where

$$\boldsymbol{\tau} = -\frac{1}{2}\boldsymbol{\chi}, \tag{42}$$

$$\boldsymbol{\chi} = \left[\|\boldsymbol{\Omega}^{\mathrm{T}}\boldsymbol{\Omega} + \boldsymbol{\Delta}^{\mathrm{T}}\boldsymbol{K}_1^{-1}\boldsymbol{\Delta} + 2\boldsymbol{K}_1\| + \frac{2}{\gamma^2} + \frac{2(\|\hat{\boldsymbol{\ell}}\| + \varepsilon_N)}{\|\boldsymbol{x}\|}\right]\boldsymbol{x}, \tag{43}$$

$$\boldsymbol{\Omega} = \frac{1}{\sqrt{c}}\boldsymbol{K}^{1/2}\Big[c\boldsymbol{K}^{-1} + \boldsymbol{\omega}^{\times}\hat{\boldsymbol{J}} - \frac{1}{2}\hat{\boldsymbol{J}}\boldsymbol{K}(q_0\boldsymbol{I}_3 + \boldsymbol{q}^{\times}) - \boldsymbol{r}_2(\boldsymbol{q}, q_0, \boldsymbol{\omega})\Big]^{\mathrm{T}}, \tag{44}$$

$$\boldsymbol{\Delta} = \Big[-\boldsymbol{\omega}^{\times}\hat{\boldsymbol{J}} + \frac{1}{2}\hat{\boldsymbol{J}}\boldsymbol{K}(q_0\boldsymbol{I}_3 + \boldsymbol{q}^{\times}) + \boldsymbol{r}_2(\boldsymbol{q}, q_0, \boldsymbol{\omega})\Big], \tag{45}$$

$\gamma > 0$ is given, $\boldsymbol{\Pi} \in \mathbf{R}^{3\times3}$, $\boldsymbol{\Gamma} \in \mathbf{R}^{3\times3}$, $\boldsymbol{K} \in \mathbf{R}^{3\times3}$ and $\boldsymbol{K}_1 \in \mathbf{R}^{3\times3}$ are the positive definite symmetric matrices, $\varepsilon_N > 0$ satisfies $\|\boldsymbol{\varepsilon}(\boldsymbol{z})\| \leqslant \varepsilon_N$, c is an adjustable parameter satisfying $c > 0$, $\hat{\boldsymbol{J}}$ is the estimate of $\boldsymbol{J}$, and the matrices or vectors $\boldsymbol{J_\sigma}$, $\boldsymbol{\phi}(\boldsymbol{\omega})$, $\boldsymbol{\varphi}(\boldsymbol{q}, q_0, \boldsymbol{\omega})$, $\boldsymbol{r}_1(\boldsymbol{\omega})$ and $\boldsymbol{r}_2(\boldsymbol{q}, q_0, \boldsymbol{\omega})$ are defined in Eqs. (29)—(33), respectively. Then if there exist $\beta > 0$ and $\rho > 0$, c, $\boldsymbol{K}$, $\boldsymbol{K}_1$ and $\lambda_{\boldsymbol{\xi}}$ satisfy the following inequalities

$$\boldsymbol{\xi}^{\mathrm{T}}\boldsymbol{PBKq} \leqslant 2\rho\|\boldsymbol{\xi}\|\|\boldsymbol{q}\|, \tag{46}$$

$$\boldsymbol{x}^{\mathrm{T}}[\boldsymbol{\sigma}^{\mathrm{T}}\boldsymbol{E} \quad \boldsymbol{\sigma}^{\mathrm{T}}\boldsymbol{D} - \boldsymbol{K}\boldsymbol{q}^{\times}\boldsymbol{\sigma}^{\mathrm{T}}]\boldsymbol{\xi} + \boldsymbol{\xi}^{\mathrm{T}}\boldsymbol{PBx} \leqslant 2\beta\|\boldsymbol{x}\|\|\boldsymbol{\xi}\|, \tag{47}$$

$$\boldsymbol{\Lambda} = \begin{bmatrix} \dfrac{c}{2}\lambda_{\boldsymbol{K}}^{\min} & 0 & -\rho \\ 0 & \dfrac{1}{2}\lambda_{\boldsymbol{K}_1}^{\min} & -\beta \\ -\rho & -\beta & \lambda_{\boldsymbol{\xi}} \end{bmatrix}, \tag{48}$$

where $\lambda_{\boldsymbol{K}}^{\min}$, $\lambda_{\boldsymbol{K}_1}^{\min}$ and $\lambda_{\boldsymbol{\xi}}$ are the minimum eigenvalues of matrices $\boldsymbol{K}$, $\boldsymbol{K}_1$ and $\boldsymbol{\xi}$, respectively; the dynamic feedback control $\boldsymbol{u}$ in Eq. (39) together with the adaptive parameter update laws in Eqs. (40) and (41) can adaptively stabilize the auxiliary system in Eqs. (2), (24) and (38), that is, $\lim\limits_{t\to\infty}\boldsymbol{q} = \boldsymbol{0}$, $\lim\limits_{t\to0}\boldsymbol{\omega} = \boldsymbol{0}$, $\lim\limits_{t\to0}\boldsymbol{\eta} = \boldsymbol{0}$ and $\lim\limits_{t\to0}\dot{\boldsymbol{\eta}} = \boldsymbol{0}$ for all initial conditions.

Proof Since $\boldsymbol{A}$ defined in Eq. (25) has all its eigenvalues in the left-hand plane, for every fixed $\lambda_{\boldsymbol{\xi}} > 0$ there exists a symmetric and positive definite solution $\boldsymbol{P} \in \mathbf{R}^{2N\times2N}$ of the Sylvester equation

$$(\boldsymbol{PA} + \boldsymbol{A}^{\mathrm{T}}\boldsymbol{P})/2 = -\lambda_{\boldsymbol{\xi}}\boldsymbol{I}, \tag{49}$$

given by

$$\boldsymbol{P} = \lambda_{\boldsymbol{\xi}}\tilde{\boldsymbol{P}} \tag{50}$$

with

$$\tilde{\boldsymbol{P}} = \begin{bmatrix} \boldsymbol{D}^{-1} + \boldsymbol{E}^{-1}\boldsymbol{D} + \boldsymbol{E}\boldsymbol{D}^{-1} & \boldsymbol{E}^{-1} \\ \boldsymbol{E}^{-1} & \boldsymbol{D}^{-1} + \boldsymbol{E}^{-1}\boldsymbol{D}^{-1} \end{bmatrix}.$$

Consider the smooth positive definite radially-unbounded Lyapunov function as follows:

$$V = \frac{1}{2}\boldsymbol{z}^{\mathrm{T}}\boldsymbol{\Theta}\boldsymbol{z} + \frac{1}{2}\tilde{\boldsymbol{\vartheta}}^{\mathrm{T}}\boldsymbol{\Pi}^{-1}\tilde{\boldsymbol{\vartheta}} + \frac{1}{2}\mathrm{tr}(\tilde{\boldsymbol{\psi}}^{\mathrm{T}}\boldsymbol{\Gamma}^{-1}\tilde{\boldsymbol{\psi}}), \tag{51}$$

where $\boldsymbol{\Theta}$ is positive definite symmetric matrix given by

$$\boldsymbol{\Theta} = \begin{bmatrix} c & \boldsymbol{0}_{1\times3} & \boldsymbol{0}_{1\times3} & \boldsymbol{0}_{1\times2N} \\ \boldsymbol{0}_{3\times1} & c\boldsymbol{I}_3 & \boldsymbol{0}_{3\times3} & \boldsymbol{0}_{3\times2N} \\ \boldsymbol{0}_{3\times1} & \boldsymbol{0}_{3\times3} & \boldsymbol{J_\sigma} & \boldsymbol{0}_{3\times2N} \\ \boldsymbol{0}_{2N\times1} & \boldsymbol{0}_{2N\times3} & \boldsymbol{0}_{2N\times3} & \boldsymbol{P} \end{bmatrix}. \tag{52}$$

Based on Eqs. (30), (31), (44), (45) and (49), the time derivate of V along Eqs. (2), (24) and (38) is

$$\begin{aligned}\dot{V} = & -c\boldsymbol{q}^{\mathrm{T}}\boldsymbol{Kq} + \boldsymbol{x}^{\mathrm{T}}\Big[c\boldsymbol{q} + \big(\boldsymbol{\phi}(\boldsymbol{\omega}) + \boldsymbol{\varphi}(\boldsymbol{q}, q_0, \boldsymbol{\omega})\big)\boldsymbol{\vartheta} + \boldsymbol{r}_1(\boldsymbol{\omega})\boldsymbol{\xi} + \boldsymbol{r}_2(\boldsymbol{q}, q_0, \boldsymbol{\omega})\boldsymbol{\omega} + \boldsymbol{\tau} + \boldsymbol{\ell} + \frac{\boldsymbol{x}}{\gamma^2}\Big] + \\ & \boldsymbol{\xi}^{\mathrm{T}}\boldsymbol{P}(\boldsymbol{A\xi} + \boldsymbol{B\omega}) + \tilde{\boldsymbol{\vartheta}}^{\mathrm{T}}\big[-\big(\boldsymbol{\phi}(\boldsymbol{\omega}) + \boldsymbol{\varphi}(\boldsymbol{q}, q_0, \boldsymbol{\omega})\big)\boldsymbol{x}\big] + \mathrm{tr}\big[\tilde{\boldsymbol{\psi}}(-\boldsymbol{S}(\boldsymbol{x})\boldsymbol{x}^{\mathrm{T}})\big] = \\ & -c\boldsymbol{q}^{\mathrm{T}}\boldsymbol{Kq} + \boldsymbol{x}^{\mathrm{T}}\Big[c\boldsymbol{q} + \big(\boldsymbol{\phi}(\boldsymbol{\omega}) + \boldsymbol{\varphi}(\boldsymbol{q}, q_0, \boldsymbol{\omega})\big)\hat{\boldsymbol{\vartheta}} + \boldsymbol{r}_1(\boldsymbol{\omega})\boldsymbol{\xi} + \boldsymbol{r}_2(\boldsymbol{q}, q_0, \boldsymbol{\omega})\boldsymbol{\omega} + \boldsymbol{\tau} + \boldsymbol{\ell} + \boldsymbol{\varepsilon} + \frac{\boldsymbol{x}}{\gamma^2}\Big] - \\ & \boldsymbol{\lambda}_{\xi}\boldsymbol{\xi}^{\mathrm{T}}\boldsymbol{\xi} + \boldsymbol{\xi}^{\mathrm{T}}\boldsymbol{PB\omega} - \boldsymbol{x}^{\mathrm{T}}(\tilde{\boldsymbol{\psi}}^{\mathrm{T}}\boldsymbol{S}(\boldsymbol{x})) = \\ & -c\boldsymbol{q}^{\mathrm{T}}\boldsymbol{Kq} - \lambda_{\boldsymbol{\xi}}\boldsymbol{\xi}^{\mathrm{T}}\boldsymbol{\xi} + \boldsymbol{x}^{\mathrm{T}}\Big[c\boldsymbol{q} - \boldsymbol{\omega}^{\times}\hat{\boldsymbol{J}}(\boldsymbol{x} - \boldsymbol{Kq}) + \\ & \frac{1}{2}\hat{\boldsymbol{J}}\boldsymbol{K}(q_0\boldsymbol{I}_3 + \boldsymbol{q}^{\times})(\boldsymbol{x} - \boldsymbol{Kq}) + \boldsymbol{r}_1(\boldsymbol{\omega})\boldsymbol{\xi} +\end{aligned}$$

$$\begin{aligned}&\boldsymbol{r}_2(\boldsymbol{q},q_0,\boldsymbol{\omega})(\boldsymbol{x}-\boldsymbol{K}\boldsymbol{q})+\boldsymbol{\tau}+\hat{\boldsymbol{\ell}}+\boldsymbol{\varepsilon}+\frac{\boldsymbol{x}}{\gamma^2}\Big]+\\&\boldsymbol{\xi}^{\mathrm{T}}\boldsymbol{P}\boldsymbol{B}(\boldsymbol{x}-\boldsymbol{K}\boldsymbol{q})=\\&-c\boldsymbol{q}^{\mathrm{T}}\boldsymbol{K}\boldsymbol{q}-\lambda_{\boldsymbol{\xi}}\boldsymbol{\xi}^{\mathrm{T}}\boldsymbol{\xi}+\boldsymbol{x}^{\mathrm{T}}\Big[c\boldsymbol{K}^{-1}+\boldsymbol{\omega}^{\times}\hat{\boldsymbol{J}}-\\&\frac{1}{2}\hat{\boldsymbol{J}}\boldsymbol{K}(q_0\boldsymbol{I}_3+\boldsymbol{q}^{\times})-\boldsymbol{r}_2(\boldsymbol{q},q_0,\boldsymbol{\omega})\Big]\boldsymbol{K}\boldsymbol{q}+\\&\boldsymbol{x}^{\mathrm{T}}\left[-\boldsymbol{\omega}^{\times}\hat{\boldsymbol{J}}+\frac{1}{2}\hat{\boldsymbol{J}}\boldsymbol{K}(q_0\boldsymbol{I}_3+\boldsymbol{q}^{\times})+\boldsymbol{r}_2(\boldsymbol{q},q_0,\boldsymbol{\omega})\right]\boldsymbol{x}+\\&\boldsymbol{x}^{\mathrm{T}}\boldsymbol{r}_1(\boldsymbol{\omega})\boldsymbol{\xi}+\boldsymbol{\xi}^{\mathrm{T}}\boldsymbol{P}\boldsymbol{B}\boldsymbol{x}-\boldsymbol{\xi}^{\mathrm{T}}\boldsymbol{P}\boldsymbol{B}\boldsymbol{K}\boldsymbol{q}+\\&\boldsymbol{x}^{\mathrm{T}}(\boldsymbol{\tau}+\hat{\boldsymbol{\ell}}+\boldsymbol{\varepsilon})+\frac{1}{\gamma^2}\boldsymbol{x}^{\mathrm{T}}\boldsymbol{x}=\\&-c\boldsymbol{q}^{\mathrm{T}}\boldsymbol{K}\boldsymbol{q}-\lambda_{\boldsymbol{\xi}}\boldsymbol{\xi}^{\mathrm{T}}\boldsymbol{\xi}+\boldsymbol{x}^{\mathrm{T}}(\boldsymbol{\tau}+\hat{\boldsymbol{\ell}}+\boldsymbol{\varepsilon})+\\&\sqrt{c}\boldsymbol{x}^{\mathrm{T}}\boldsymbol{\Omega}^{\mathrm{T}}\boldsymbol{K}^{1/2}\boldsymbol{q}+\boldsymbol{x}^{\mathrm{T}}\boldsymbol{\Delta}\boldsymbol{x}+\boldsymbol{x}^{\mathrm{T}}\boldsymbol{r}_1(\boldsymbol{\omega})\boldsymbol{\xi}+\\&\boldsymbol{\xi}^{\mathrm{T}}\boldsymbol{P}\boldsymbol{B}\boldsymbol{x}-\boldsymbol{\xi}^{\mathrm{T}}\boldsymbol{P}\boldsymbol{B}\boldsymbol{K}\boldsymbol{q}+\frac{1}{\gamma^2}\boldsymbol{x}^{\mathrm{T}}\boldsymbol{x}.\end{aligned}\tag{53}$$

Substituting Eq. (42) into Eq. (53) yields

$$\begin{aligned}\dot{V}\leqslant&-\frac{c}{2}\boldsymbol{q}^{\mathrm{T}}\boldsymbol{K}\boldsymbol{q}-\lambda_{\boldsymbol{\xi}}\boldsymbol{\xi}^{\mathrm{T}}\boldsymbol{\xi}-\frac{1}{2}\boldsymbol{x}^{\mathrm{T}}\boldsymbol{K}_1\boldsymbol{x}-\\&\frac{1}{2}\|\sqrt{c}\boldsymbol{K}^{1/2}\boldsymbol{q}-\boldsymbol{\Omega}\boldsymbol{x}\|^2-\\&\frac{1}{2}\boldsymbol{x}^{\mathrm{T}}(\boldsymbol{K}_1-\boldsymbol{\Delta})^{\mathrm{T}}\boldsymbol{K}_1^{-1}(\boldsymbol{K}_1-\boldsymbol{\Delta})\boldsymbol{x}+\\&\boldsymbol{x}^{\mathrm{T}}\boldsymbol{r}_1(\boldsymbol{\omega})\boldsymbol{\xi}+\boldsymbol{\xi}^{\mathrm{T}}\boldsymbol{P}\boldsymbol{B}\boldsymbol{x}-\boldsymbol{\xi}^{\mathrm{T}}\boldsymbol{P}\boldsymbol{B}\boldsymbol{K}\boldsymbol{q}.\end{aligned}\tag{54}$$

Note that

$$\boldsymbol{x}^{\mathrm{T}}[\boldsymbol{0}\quad-\boldsymbol{x}^{\times}\boldsymbol{\sigma}^{\mathrm{T}}]\boldsymbol{\xi}=\boldsymbol{0}.$$

Therefore, we have

$$\boldsymbol{x}^{\mathrm{T}}\boldsymbol{r}_1(\boldsymbol{\omega})\boldsymbol{\xi}=\boldsymbol{x}^{\mathrm{T}}[\boldsymbol{\sigma}^{\mathrm{T}}\boldsymbol{E}\quad\boldsymbol{\sigma}^{\mathrm{T}}\boldsymbol{D}-\boldsymbol{K}\boldsymbol{q}^{\times}\boldsymbol{\sigma}^{\mathrm{T}}]\boldsymbol{\xi}.$$

If Inequalities (46) and (47) hold, we have

$$\begin{aligned}\dot{V}\leqslant&-\frac{c}{2}\lambda_{\boldsymbol{K}}^{\min}\|\boldsymbol{q}\|^2-\lambda_{\boldsymbol{\xi}}\|\boldsymbol{\xi}\|^2-\frac{1}{2}\lambda_{\boldsymbol{K}_1}^{\min}\|\boldsymbol{x}\|^2-\\&\frac{1}{2}\|\sqrt{c}\boldsymbol{K}^{1/2}\boldsymbol{q}-\boldsymbol{\Omega}\boldsymbol{x}\|^2-\\&\frac{1}{2}\boldsymbol{x}^{\mathrm{T}}(\boldsymbol{K}_1-\boldsymbol{\Delta})^{\mathrm{T}}\boldsymbol{K}_1^{-1}(\boldsymbol{K}_1-\boldsymbol{\Delta})\boldsymbol{x}+\\&2\rho\|\boldsymbol{\xi}\|\|\boldsymbol{q}\|+2\boldsymbol{\beta}\|\boldsymbol{x}\|\|\boldsymbol{\xi}\|\leqslant\\&-\frac{c}{2}\lambda_{\boldsymbol{K}}^{\min}\|\boldsymbol{q}\|^2-\frac{1}{2}\lambda_{\boldsymbol{K}_1}^{\min}\|\boldsymbol{x}\|^2-\lambda_{\xi}\|\boldsymbol{\xi}\|^2+\\&2\rho\|\boldsymbol{\xi}\|\|\boldsymbol{q}\|+2\boldsymbol{\beta}\|\boldsymbol{x}\|\|\boldsymbol{\xi}\|\leqslant\\&-\left[\|\boldsymbol{q}\|\quad\|\boldsymbol{x}\|\quad\|\boldsymbol{\xi}\|\right]\boldsymbol{\Lambda}\begin{bmatrix}\|\boldsymbol{q}\|\\\|\boldsymbol{x}\|\\\|\boldsymbol{\xi}\|\end{bmatrix}.\end{aligned}\tag{55}$$

Here the matrix $\boldsymbol{\Lambda}$ is defined in Eq. (48). Then if $\boldsymbol{\Lambda}$ is positive definite, i.e., there exists a triplet of positive parameters $(\lambda_{\boldsymbol{K}}^{\min},\lambda_{\boldsymbol{K}_1}^{\min},\lambda_{\boldsymbol{\xi}})$ such that the following conditions are satisfied

$$\frac{1}{2}\lambda_{\boldsymbol{K}_1}^{\min}>\beta^2/\lambda_{\boldsymbol{\xi}},\tag{56}$$

$$\|\boldsymbol{\Lambda}\|=\frac{c}{2}\lambda_{\boldsymbol{K}}^{\min}\Big(\frac{1}{2}\lambda_{\boldsymbol{K}_1}^{\min}\lambda_{\boldsymbol{\xi}}-\beta^2\Big)-\frac{1}{2}\rho^2\lambda_{\boldsymbol{K}_1}^{\min}>0,\tag{57}$$

we have

$$\dot{V}\leqslant-\lambda_{\boldsymbol{\Lambda}}^{\min}(\|\boldsymbol{q}\|^2+\|\boldsymbol{x}\|^2+\|\boldsymbol{\xi}\|^2),\tag{58}$$

where $\lambda_{\boldsymbol{\Lambda}}^{\min}>0$ is the minimum eigenvalue of matrix $\boldsymbol{\Lambda}$. It follows from the Barbalat's theorem[33] that $\boldsymbol{q}\to\boldsymbol{0}$, $\boldsymbol{x}\to\boldsymbol{0}$ and $\boldsymbol{\xi}\to\boldsymbol{0}$, and therefore $\boldsymbol{\omega}\to\boldsymbol{0}$, $\boldsymbol{\eta}\to\boldsymbol{0}$ and $\dot{\boldsymbol{\eta}}\to\boldsymbol{0}$ as $t\to\infty$ based on Remark 4.

Theorem 2 Suppose that Assumptions 1—4 are satisfied. Then the dynamic feedback control law

$$\begin{aligned}\boldsymbol{u}=&\boldsymbol{\alpha}^*(\boldsymbol{q},q_0,\boldsymbol{\omega},\hat{\boldsymbol{\vartheta}},\boldsymbol{\tau}_{\max})=\\&-2\boldsymbol{R}^{-1}(\boldsymbol{q},q_0,\boldsymbol{\omega},\hat{\boldsymbol{\vartheta}},\boldsymbol{\tau}_{\max})\boldsymbol{x}=\\&\begin{cases}-\dfrac{\tau_{\max}\boldsymbol{x}}{\|\boldsymbol{x}\|}, & \|\boldsymbol{\tau}\|>\tau_{\max}\\ \boldsymbol{\tau}, & \|\boldsymbol{\tau}\|\leqslant\tau_{\max}\end{cases}\end{aligned}\tag{59}$$

together with the adaptive parameter update laws given in Eqs. (40) and (41), where $\boldsymbol{\tau}=-\boldsymbol{\chi}$ and $\boldsymbol{\chi}$ is defined in Eq. (43), for some given $\gamma>0$, can solve the H_∞ inverse optimal assignment problem for the fault-free attitude control system in Eqs. (2), (24) and (28) with $\boldsymbol{f}=\boldsymbol{0}_{3\times1}$ and $\boldsymbol{\delta}=\boldsymbol{I}_3$ in the whole process of attitude control by minimizing the cost functional

$$\begin{aligned}L_a=\lim_{t\to\infty}\Bigg\{&4V(t)+\int_0^t\Big[l(\boldsymbol{q},q_0,\boldsymbol{\omega},\hat{\boldsymbol{\vartheta}},\boldsymbol{\xi})+\\&\boldsymbol{u}^{\mathrm{T}}\boldsymbol{R}\boldsymbol{u}-\gamma^2\|\boldsymbol{d}\|^2\Big]\mathrm{d}\kappa\Bigg\},\end{aligned}\tag{60}$$

for each $\boldsymbol{\vartheta}\in\mathbf{R}^6$, where

$$\begin{aligned}&l(\boldsymbol{q},q_0,\boldsymbol{\omega},\hat{\boldsymbol{\vartheta}},\boldsymbol{\xi})=\\&\quad-4\big\{c\boldsymbol{q}^{\mathrm{T}}\boldsymbol{\omega}+\boldsymbol{x}^{\mathrm{T}}\big[(\boldsymbol{\phi}(\boldsymbol{\omega})+\boldsymbol{\varphi}(\boldsymbol{q},q_0,\boldsymbol{\omega}))\hat{\boldsymbol{\vartheta}}+\\&\quad\boldsymbol{r}_1(\boldsymbol{\omega})\boldsymbol{\xi}+\boldsymbol{r}_2(\boldsymbol{q},q_0,\boldsymbol{\omega})\boldsymbol{\omega}\big]+\boldsymbol{\xi}^{\mathrm{T}}\boldsymbol{P}(\boldsymbol{A}\boldsymbol{\xi}+\boldsymbol{B}\boldsymbol{\omega})\big\}+\\&\quad4\boldsymbol{x}^{\mathrm{T}}\boldsymbol{R}^{-1}\boldsymbol{x}-\frac{4}{\gamma^2}\boldsymbol{x}^{\mathrm{T}}\boldsymbol{x}.\end{aligned}\tag{61}$$

Proof From the definition of $l(\boldsymbol{q},q_0,\boldsymbol{\omega},\hat{\boldsymbol{\vartheta}},\boldsymbol{\xi})$ in Eq. (61) and the proof of Theorem 1, we have

$$\begin{aligned}&l(\boldsymbol{q},q_0,\boldsymbol{\omega},\hat{\boldsymbol{\vartheta}},\boldsymbol{\xi})=\\&\quad-4\Big\{c\boldsymbol{q}^{\mathrm{T}}\boldsymbol{\omega}+\boldsymbol{x}^{\mathrm{T}}\big[(\boldsymbol{\phi}(\boldsymbol{\omega})+\boldsymbol{\varphi}(\boldsymbol{q},q_0,\boldsymbol{\omega}))\hat{\boldsymbol{\vartheta}}+\\&\quad\boldsymbol{r}_1(\boldsymbol{\omega})\boldsymbol{\xi}+\boldsymbol{r}_2(\boldsymbol{q},q_0,\boldsymbol{\omega})\boldsymbol{\omega}\big]+\\&\quad\boldsymbol{\xi}^{\mathrm{T}}\boldsymbol{P}(\boldsymbol{A}\boldsymbol{\xi}+\boldsymbol{B}\boldsymbol{\omega})-\boldsymbol{R}^{-1}\boldsymbol{x}+\frac{\boldsymbol{x}^{\mathrm{T}}\boldsymbol{x}}{\gamma^2}\Big\}\geqslant\\&\quad4\lambda_{\boldsymbol{\Lambda}}^{\min}(\|\boldsymbol{q}\|^2+\|\boldsymbol{x}\|^2+\|\boldsymbol{\xi}\|^2),\end{aligned}$$

from which we observe that $l(\boldsymbol{q}, q_0, \boldsymbol{\omega}, \hat{\boldsymbol{\vartheta}}, \boldsymbol{\xi})$ is positive definite in $\boldsymbol{q}$, q_0, $\boldsymbol{\omega}$, $\hat{\boldsymbol{\vartheta}}$ and $\boldsymbol{\xi}$ for each $\boldsymbol{\vartheta} \in \mathbf{R}^6$. Therefore, the cost functional L_a in Eq. (60) is a meaningful cost functional, penalizing $\boldsymbol{q}$, q_0, $\boldsymbol{\omega}$, $\hat{\boldsymbol{\vartheta}}$ and $\boldsymbol{\xi}$ as well as the control effort $\boldsymbol{u}$. Next, we prove that the control law in Eq. (59) with Eqs. (40) and (41) minimizes the cost functional in Eq. (60).

$$\begin{aligned}
L_a = & \lim_{t\to\infty}\left\{4V(t) + \int_0^t \Big[-4\Big(c\boldsymbol{q}^{\mathrm{T}}\boldsymbol{\omega} + \right. \\
& \boldsymbol{x}^{\mathrm{T}}((\boldsymbol{\phi}(\boldsymbol{\omega}) + \boldsymbol{\varphi}(\boldsymbol{q}, q_0, \boldsymbol{\omega}))\hat{\boldsymbol{\vartheta}} + \\
& \boldsymbol{r}_1(\boldsymbol{\omega})\boldsymbol{\xi} + \boldsymbol{r}_2(\boldsymbol{q}, q_0, \boldsymbol{\omega})\boldsymbol{\omega}) + \boldsymbol{\xi}^{\mathrm{T}}\boldsymbol{P}(\boldsymbol{A}\boldsymbol{\xi} + \boldsymbol{B}\boldsymbol{\omega})\Big) + \\
& \left. 4\boldsymbol{x}^{\mathrm{T}}\boldsymbol{R}^{-1}\boldsymbol{x} - \frac{4}{\gamma^2}\boldsymbol{x}^{\mathrm{T}}\boldsymbol{x} + \boldsymbol{u}^{\mathrm{T}}\boldsymbol{R}\boldsymbol{u} - \gamma^2\|\boldsymbol{d}\|^2\Big]\mathrm{d}\kappa\right\} = \\
& \lim_{t\to\infty}\left\{-4\int_0^t \Big[c\boldsymbol{q}^{\mathrm{T}}\boldsymbol{\omega} + \boldsymbol{x}^{\mathrm{T}}\Big((\boldsymbol{\phi}(\boldsymbol{\omega}) + \boldsymbol{\varphi}(\boldsymbol{q}, q_0, \boldsymbol{\omega}))\boldsymbol{\vartheta} + \right. \\
& \boldsymbol{r}_1(\boldsymbol{\omega})\boldsymbol{\xi} + \boldsymbol{r}_2(\boldsymbol{q}, q_0, \boldsymbol{\omega})\boldsymbol{\omega} + \boldsymbol{d} + \boldsymbol{u}\Big) + \\
& \boldsymbol{x}^{\mathrm{T}}\Big(-(\boldsymbol{F}(\boldsymbol{\omega}) + \boldsymbol{G}(\boldsymbol{q}, q_0, \boldsymbol{\omega}))^{\mathrm{T}}\tilde{\boldsymbol{\vartheta}}\Big) + \\
& \boldsymbol{\xi}^{\mathrm{T}}\boldsymbol{P}(\boldsymbol{A}\xi + \boldsymbol{B}\boldsymbol{\omega})\Big]\mathrm{d}\kappa - \\
& \int_0^t \Big(\frac{4\boldsymbol{x}^{\mathrm{T}}\boldsymbol{x}}{\gamma^2} - 4\boldsymbol{x}^{\mathrm{T}}\boldsymbol{d} + \gamma^2\|\boldsymbol{d}\|^2\Big)\mathrm{d}\kappa + \\
& \left. \int_0^t (\boldsymbol{u}^{\mathrm{T}}\boldsymbol{R}\boldsymbol{u} + 4\boldsymbol{x}^{\mathrm{T}}\boldsymbol{u} + 4\boldsymbol{x}^{\mathrm{T}}\boldsymbol{R}^{-1}\boldsymbol{x})\mathrm{d}\kappa + 4V(t)\right\} = \\
& \lim_{t\to\infty}\Big[4V(t) - 4\int_0^t \frac{\mathrm{d}}{\mathrm{d}t}\Big(c\boldsymbol{q}^{\mathrm{T}}\boldsymbol{q} + c(1-q_0)^2 + \\
& \frac{1}{2}\boldsymbol{x}^{\mathrm{T}}\boldsymbol{J}_{\boldsymbol{\sigma}}\boldsymbol{x} + \frac{1}{2}\tilde{\boldsymbol{\vartheta}}^{\mathrm{T}}\boldsymbol{T}^{-1}\tilde{\boldsymbol{\vartheta}} + \frac{1}{2}\boldsymbol{\xi}^{\mathrm{T}}\boldsymbol{P}\boldsymbol{\xi}\Big)\mathrm{d}\kappa - \\
& 2\int_0^t \Big(\frac{2\boldsymbol{x}^{\mathrm{T}}\boldsymbol{x}}{\gamma^2} - 2\boldsymbol{x}^{\mathrm{T}}\boldsymbol{d} + \frac{\gamma^2\|\boldsymbol{d}\|^2}{2}\Big)\mathrm{d}\kappa + \\
& \int_0^t (\boldsymbol{u} - \boldsymbol{\alpha}^*)^{\mathrm{T}}\boldsymbol{R}(\boldsymbol{u} - \boldsymbol{\alpha}^*)\mathrm{d}\kappa\Big] = \\
& \lim_{t\to\infty}\Big[4V(0) - 2\int_0^t \Big(\frac{\sqrt{2}\boldsymbol{x}}{\gamma} - \frac{\gamma}{\sqrt{2}}\boldsymbol{d}\Big)^{\mathrm{T}} \times \\
& \Big(\frac{\sqrt{2}\boldsymbol{x}}{\gamma} - \frac{\gamma}{\sqrt{2}}\boldsymbol{d}\Big)\mathrm{d}\kappa + \\
& \int_0^t (\boldsymbol{u} - \boldsymbol{\alpha}^*)^{\mathrm{T}}\boldsymbol{R}(\boldsymbol{u} - \boldsymbol{\alpha}^*)\mathrm{d}\kappa\Big].
\end{aligned} \tag{62}$$

The "worst-case" disturbance is $\boldsymbol{d}^* = \dfrac{2\boldsymbol{x}}{\gamma^2}$, and the minimum of Eq. (60) is $L_a^* = 4V(0)$ with $\boldsymbol{u} = \boldsymbol{\alpha}^*$. To this end, from the controller in Eq. (59), the inequality $\|\boldsymbol{u}\| \leqslant \left\|\dfrac{\tau_{\max}\boldsymbol{x}}{\|\boldsymbol{x}\|}\right\| \leqslant \tau_{\max}$ can be obtained. The proof is completed.

Remark 5 Based on the control law given in Eq. (59), the parameters c, $\boldsymbol{K}$ and $\boldsymbol{K}_1$ can be determined. Note that given a spacecraft with certain structural properties, it is always possible to fix values $\lambda_{\boldsymbol{\xi}}$, c and a matrix $\boldsymbol{K}$, and accordingly determine the values for β, ρ based on Inequalities (46) and (47) such that the conditions (Eqs. (56) and (57)) can be satisfied by the appropriate gain matrix $\boldsymbol{K}_1$.

Remark 6 In the proof of Theorem 2, we establish that the resulting closed-loop system renders the cost functional in Eq. (60) meaningful and guarantees that the constrained controller in Eq. (59) with Eqs. (40) and (41) is optimal with respect to the cost under Assumptions 1—4.

Remark 7 This proposed H_∞ inverse optimal adaptive approach for flexible spacecraft with input saturation is greatly inspired by Theorem 6 of Ref. [26]. However, the method addressed by Luo et al.[26] was limited only to handling rigid spacecraft and did not explicitly consider the influence of flexible vibration in attitude control, and thereby could hardly be directly extended to the flexible spacecraft system as mentioned in the introduction. In addition, the control input saturation was also not taken into account in Ref. [26] to implement the control law, which may result in performance deterioration or even instability of the system in the actual control.

Remark 8 A discontinuous projection[34] is employed to modify the adaption law in Eq. (40) to avoid the divergence of the estimates of the parameters by a small disturbance in the updating law, that is

$$\dot{\hat{\boldsymbol{\vartheta}}}_i = \mathrm{Proj}_{\hat{\boldsymbol{\vartheta}}_i}\{\boldsymbol{\Pi}[\boldsymbol{\phi}(\boldsymbol{\omega}) + \boldsymbol{\varphi}(\boldsymbol{q}, q_0, \boldsymbol{\omega})]^{\mathrm{T}}(\boldsymbol{\omega} + \boldsymbol{K}\boldsymbol{q})\}, \quad i = 1, 2, \cdots, 6,$$

where the projection mapping operator is defined as

$$\mathrm{Proj}_e(\hbar) = \begin{cases} 0, & e = e_{\max} \ \text{and} \ \hbar < 0 \\ -\hbar, & e_{\min} < e < e_{\max}, \ e = e_{\min} \\ & \text{and} \ \hbar \geqslant 0, \ \ e = e_{\min} \ \text{and} \ \hbar \leqslant 0 \\ 0, & e = e_{\min} \ \text{and} \ \hbar > 0 \end{cases}; \tag{63}$$

$e_{\min}$ and $e_{\max}$ are the known constants.

2.2.2 *Inverse Optimal Adaptive Fault-Tolerant Controller (IOAFTC) Design Under Actuator Faults*

The proposed constrained control law in Eq. (59) can achieve the asymptotical stability of the resulting closed-loop attitude system and is optimal with respect to the cost functional in Eq. (60) with fault-free actuators. However, when actuator fault occurs, it will not ensure the stabilization and accuracy for the attitude control system in Eqs. (2), (24) and (28). Therefore, a fault-tolerant controller design is required for the flexible spacecraft with actuator faults. In this section, the additive faults and the partial loss of actuator effectiveness are considered simultaneously to design the attitude controller for the flexible spacecraft in the presence of control input saturation, uncertainty inertia matrix and external disturbances. An inverse optimal adaptive control method is employed to design a robust and optimal controller against actuator faults and external disturbances. In this section, $\boldsymbol{\ell}$ is redefined as follows:

$$\boldsymbol{\ell}=\frac{1}{\hat{\mu}}(\boldsymbol{u}-\boldsymbol{\tau}), \tag{64}$$

where $1/\hat{\mu}$ is the parameter estimate of μ in Eq. (6) with the estimate error defined by $\tilde{\mu}=1/\hat{\mu}-\mu$.

Theorem 3 Consider an auxiliary system that consists of Eqs. (2), (24) and the following equation

$$\begin{aligned}\boldsymbol{J}_{\boldsymbol{\sigma}}\dot{\boldsymbol{x}}=&\left[\boldsymbol{\phi}(\boldsymbol{\omega})+\boldsymbol{\varphi}(\boldsymbol{q},q_0,\boldsymbol{\omega})\right]\boldsymbol{\vartheta}+\boldsymbol{r}_1(\boldsymbol{\omega})\boldsymbol{\xi}+\\&\boldsymbol{r}_2(\boldsymbol{q},q_0,\boldsymbol{\omega})\boldsymbol{\omega}+\boldsymbol{\delta u}+\frac{\boldsymbol{x}}{\gamma^2},\end{aligned} \tag{65}$$

for which Assumptions 1—4 hold, under the dynamic feedback control law

$$\begin{aligned}\boldsymbol{u}=&\boldsymbol{\alpha}(\boldsymbol{q},q_0,\boldsymbol{\omega},\hat{\boldsymbol{\vartheta}},\tau_{\max})=\\&-\boldsymbol{R}_1^{-1}(\boldsymbol{q},q_0,\boldsymbol{\omega},\hat{\boldsymbol{\vartheta}},\tau_{\max})\boldsymbol{x}=\\&\begin{cases}-\dfrac{\tau_{\max}\boldsymbol{x}}{2\|\boldsymbol{x}\|}, & \|\boldsymbol{\tau}\|>\dfrac{\tau_{\max}}{2}\\ \boldsymbol{\tau}, & \|\boldsymbol{\tau}\|\leqslant\dfrac{\tau_{\max}}{2}\end{cases}\end{aligned} \tag{66}$$

together with the adaptive parameter update laws

$$\dot{\hat{\mu}}=\frac{1}{2}\boldsymbol{x}^{\mathrm{T}}\hat{\mu}^3\boldsymbol{\chi}, \tag{67}$$

$$\dot{\hat{\boldsymbol{\vartheta}}}=\boldsymbol{\Pi}\boldsymbol{\pi}, \tag{68}$$

$$\dot{\hat{\boldsymbol{\psi}}}=\boldsymbol{\Gamma}\boldsymbol{S}(\boldsymbol{x})\boldsymbol{x}^{\mathrm{T}}, \tag{69}$$

where

$$\boldsymbol{\tau}(\boldsymbol{q},q_0,\boldsymbol{\omega},\hat{\boldsymbol{\vartheta}})=-\frac{1}{2}\hat{\mu}\boldsymbol{\chi},$$

$\boldsymbol{\pi}$ and $\boldsymbol{\chi}$ are defined in Eqs. (40) and (43), respectively; $\boldsymbol{\Pi}\in\mathbf{R}^{3\times3}$ and $\boldsymbol{\Gamma}\in\mathbf{R}^{3\times3}$ are the positive definite matrices. Then if β, ρ, c, $\boldsymbol{K}$, $\boldsymbol{K}_1$ and $\lambda_{\boldsymbol{\xi}}$ satisfy Inequalities (46)—(48), the dynamic feedback control $\boldsymbol{u}$ in Eq. (66) together with the adaptive parameter update laws in Eqs. (67)—(69) can adaptively stabilize the auxiliary system in Eqs. (2), (24) and (65), that is, $\lim\limits_{t\to\infty}\boldsymbol{q}=\boldsymbol{0}$, $\lim\limits_{t\to0}\boldsymbol{\omega}=\boldsymbol{0}$, $\lim\limits_{t\to0}\boldsymbol{\eta}=\boldsymbol{0}$ and $\lim\limits_{t\to0}\dot{\boldsymbol{\eta}}=\boldsymbol{0}$ for all initial conditions.

Proof Following the same steps as in Theorem 1, we consider the smooth positive definite radially-unbounded Lyapunov function as follows:

$$\begin{aligned}V_1=&\frac{1}{2}\boldsymbol{z}^{\mathrm{T}}\boldsymbol{\Theta}\boldsymbol{z}+\frac{1}{2}\tilde{\boldsymbol{\vartheta}}^{\mathrm{T}}\boldsymbol{\Pi}^{-1}\tilde{\boldsymbol{\vartheta}}+\\&\frac{1}{2}\tilde{\mu}^2+\frac{1}{2}\mathrm{tr}(\tilde{\boldsymbol{\psi}}^{\mathrm{T}}\boldsymbol{\Gamma}^{-1}\tilde{\boldsymbol{\psi}}),\end{aligned} \tag{70}$$

where positive definite symmetric matrix $\boldsymbol{\Theta}$ is defined in Eq. (52). The time derivate of V_1 along Eqs. (2), (24) and (65) is given by

$$\begin{aligned}\dot{V}_1=&-c\boldsymbol{q}^{\mathrm{T}}\boldsymbol{K}\boldsymbol{q}+\boldsymbol{x}^{\mathrm{T}}\Big\{c\boldsymbol{q}+[\boldsymbol{\phi}(\boldsymbol{\omega})+\boldsymbol{\varphi}(\boldsymbol{q},q_0,\boldsymbol{\omega})]\boldsymbol{\vartheta}+\\&\boldsymbol{r}_1(\boldsymbol{\omega})\varsigma+\boldsymbol{r}_2(\boldsymbol{q},q_0,\boldsymbol{\omega})\boldsymbol{\omega}+\boldsymbol{\delta u}+\frac{\boldsymbol{x}}{\gamma^2}\Big\}+\\&\boldsymbol{\xi}^{\mathrm{T}}\boldsymbol{P}(\boldsymbol{A\xi}+\boldsymbol{B\omega})+\tilde{\boldsymbol{\vartheta}}^{\mathrm{T}}\{-[\boldsymbol{\phi}(\boldsymbol{\omega})+\\&\boldsymbol{\varphi}(\boldsymbol{q},q_0,\boldsymbol{\omega})]\boldsymbol{x}\}-\frac{\tilde{\mu}\dot{\hat{\mu}}}{\hat{\mu}^2}+\mathrm{tr}[\tilde{\boldsymbol{\psi}}(-\boldsymbol{S}(\boldsymbol{x})\boldsymbol{x}^{\mathrm{T}})]=\\&-c\boldsymbol{q}^{\mathrm{T}}\boldsymbol{K}\boldsymbol{q}-\lambda_{\boldsymbol{\xi}}\boldsymbol{\xi}^{\mathrm{T}}\xi+\boldsymbol{x}^{\mathrm{T}}\boldsymbol{\delta u}+\sqrt{c}\boldsymbol{x}^{\mathrm{T}}\boldsymbol{\Omega}^{\mathrm{T}}\boldsymbol{K}^{1/2}\boldsymbol{q}+\\&\boldsymbol{x}^{\mathrm{T}}\boldsymbol{\Delta x}+\boldsymbol{\xi}^{\mathrm{T}}\boldsymbol{r}_1(\boldsymbol{\omega})\boldsymbol{x}+\boldsymbol{\xi}^{\mathrm{T}}\boldsymbol{PBx}-\boldsymbol{\xi}^{\mathrm{T}}\boldsymbol{PBKq}+\\&\frac{1}{\gamma^2}\boldsymbol{x}^{\mathrm{T}}\boldsymbol{x}-\frac{\tilde{\mu}\dot{\hat{\mu}}}{\hat{\mu}^2}+\mathrm{tr}[\tilde{\boldsymbol{\psi}}(-\boldsymbol{S}(\boldsymbol{x})\boldsymbol{x}^{\mathrm{T}})]\leqslant\\&-c\boldsymbol{q}^{\mathrm{T}}\boldsymbol{K}\boldsymbol{q}-\lambda_{\boldsymbol{\xi}}\boldsymbol{\xi}^{\mathrm{T}}\boldsymbol{\xi}+\boldsymbol{x}^{\mathrm{T}}\mu\boldsymbol{u}+\sqrt{c}\boldsymbol{x}^{\mathrm{T}}\boldsymbol{\Omega}^{\mathrm{T}}\boldsymbol{K}^{1/2}\boldsymbol{q}+\\&\boldsymbol{x}^{\mathrm{T}}\boldsymbol{\Delta x}+\boldsymbol{\xi}^{\mathrm{T}}\boldsymbol{r}_1(\boldsymbol{\omega})\boldsymbol{x}+\boldsymbol{\xi}^{\mathrm{T}}\boldsymbol{PBx}-\boldsymbol{\xi}^{\mathrm{T}}\boldsymbol{PBKq}+\\&\frac{1}{\gamma^2}\boldsymbol{x}^{\mathrm{T}}\boldsymbol{x}-\frac{\tilde{\mu}\dot{\hat{\mu}}}{\hat{\mu}^2}+\mathrm{tr}[\tilde{\boldsymbol{\psi}}(-\boldsymbol{S}(\boldsymbol{x})\boldsymbol{x}^{\mathrm{T}})]=\\&-c\boldsymbol{q}^{\mathrm{T}}\boldsymbol{K}\boldsymbol{q}-\lambda_{\boldsymbol{\xi}}\boldsymbol{\xi}^{\mathrm{T}}\boldsymbol{\xi}+\sqrt{c}\boldsymbol{x}^{\mathrm{T}}\boldsymbol{\Omega}^{\mathrm{T}}\boldsymbol{K}^{1/2}\boldsymbol{q}+\\&\boldsymbol{x}^{\mathrm{T}}\boldsymbol{\Delta x}+\boldsymbol{\xi}^{\mathrm{T}}\boldsymbol{r}_1(\boldsymbol{\omega})\boldsymbol{x}+\boldsymbol{\xi}^{\mathrm{T}}\boldsymbol{PBx}-\boldsymbol{\xi}^{\mathrm{T}}\boldsymbol{PBKq}+\\&\frac{1}{\gamma^2}\boldsymbol{x}^{\mathrm{T}}\boldsymbol{x}+\boldsymbol{x}^{\mathrm{T}}\mu\Big(-\frac{1}{2}\hat{\mu}\boldsymbol{\chi}+\frac{\boldsymbol{\ell}}{\boldsymbol{\mu}}\Big)-\\&\frac{1-\hat{\mu}\mu}{2\hat{\mu}}\boldsymbol{x}^{\mathrm{T}}\hat{\mu}\boldsymbol{\chi}-\boldsymbol{x}^{\mathrm{T}}(\tilde{\boldsymbol{\psi}}^{\mathrm{T}}\boldsymbol{S}(\boldsymbol{x}))=\\&-c\boldsymbol{q}^{\mathrm{T}}\boldsymbol{K}\boldsymbol{q}-\lambda_{\boldsymbol{\xi}}\boldsymbol{\xi}^{\mathrm{T}}\boldsymbol{\xi}+\sqrt{c}\boldsymbol{x}^{\mathrm{T}}\boldsymbol{\Omega}^{\mathrm{T}}\boldsymbol{K}^{1/2}\boldsymbol{q}+\\&\boldsymbol{x}^{\mathrm{T}}\boldsymbol{\Delta x}+\boldsymbol{\xi}^{\mathrm{T}}\boldsymbol{r}_1(\boldsymbol{\omega})\boldsymbol{x}+\boldsymbol{\xi}^{\mathrm{T}}\boldsymbol{PBx}-\boldsymbol{\xi}^{\mathrm{T}}\boldsymbol{PBKq}+\\&\frac{1}{\gamma^2}\boldsymbol{x}^{\mathrm{T}}\boldsymbol{x}+\boldsymbol{x}^{\mathrm{T}}\Big(-\frac{1}{2}\boldsymbol{\chi}+\boldsymbol{\ell}+\boldsymbol{\varepsilon}\Big)\leqslant\\&-\frac{c}{2}\boldsymbol{q}^{\mathrm{T}}\boldsymbol{K}\boldsymbol{q}-\lambda_{\boldsymbol{\xi}}\boldsymbol{\xi}^{\mathrm{T}}\boldsymbol{\xi}-\frac{1}{2}\boldsymbol{x}^{\mathrm{T}}\boldsymbol{K}_1\boldsymbol{x}-\\&\frac{1}{2}\|\sqrt{c}\boldsymbol{K}^{1/2}\boldsymbol{q}-\boldsymbol{\Omega x}\|^2-\\&\frac{1}{2}\boldsymbol{x}^{\mathrm{T}}(\boldsymbol{K}_1-\boldsymbol{\Delta})^{\mathrm{T}}\boldsymbol{K}_1^{-1}(\boldsymbol{K}_1-\boldsymbol{\Delta})\boldsymbol{x}+\boldsymbol{x}^{\mathrm{T}}\boldsymbol{r}_1(\boldsymbol{\omega})\boldsymbol{\xi}+\\&\boldsymbol{\xi}^{\mathrm{T}}\boldsymbol{PBx}-\boldsymbol{\xi}^{\mathrm{T}}\boldsymbol{PBKq}\leqslant\\&-\lambda_{\boldsymbol{\Lambda}}^{\min}\big(\|\boldsymbol{q}\|^2+\|\boldsymbol{x}\|^2+\|\boldsymbol{\xi}\|^2\big),\end{aligned} \tag{71}$$

where $\lambda_{\boldsymbol{\Lambda}}^{\min}>0$ is the minimum eigenvalue of matrice $\boldsymbol{\Lambda}$, and $\boldsymbol{\Lambda}$ is defined in Eq. (48). As analyzed in Theorem 1, we can conclude that, under the controller given in Eq. (66) with the adaptive parameter update laws in Eqs. (67)—(69), the auxiliary system in Eqs. (2), (24) and (65) is globally adaptively stable, that is $\boldsymbol{q}\to\boldsymbol{0}$, $\boldsymbol{x}\to\boldsymbol{0}$, $\boldsymbol{\omega}\to\boldsymbol{0}$, $\boldsymbol{\eta}\to\boldsymbol{0}$ and $\dot{\boldsymbol{\eta}}\to\boldsymbol{0}$ as $t\to\infty$.

Theorem 4 Suppose that Assumptions 1—4 are satisfied. Then the dynamic feedback control law

$$\begin{aligned}\boldsymbol{u} = &\boldsymbol{\alpha}^*(\boldsymbol{q}, q_0, \boldsymbol{\omega}, \hat{\boldsymbol{\vartheta}}, \tau_{\max}) = \\ &-2\boldsymbol{R}_1^{-1}(\boldsymbol{q}, q_0, \boldsymbol{\omega}, \hat{\boldsymbol{\vartheta}}, \tau_{\max})\boldsymbol{x} = \\ &\begin{cases} -\dfrac{\tau_{\max}\boldsymbol{x}}{\|\boldsymbol{x}\|}, & \|\boldsymbol{\tau}\| > \tau_{\max} \\ \boldsymbol{\tau}, & \|\boldsymbol{\tau}\| \leqslant \tau_{\max} \end{cases}\end{aligned} \tag{72}$$

together with the adaptive parameter update laws in Eqs. (67)—(69), where $\boldsymbol{\tau} = -\hat{\mu}\boldsymbol{\chi}$ and $\boldsymbol{\chi}$ is defined in Eq. (43), for given $\gamma > 0$, can solve the H_∞ inverse optimal control problem for the attitude control system in Eqs. (2), (24) and (28) by minimizing the cost functional

$$\begin{aligned}L_a = \lim_{t\to\infty}\Big\{4V_1(t) + \int_0^t \big[l(\boldsymbol{q}, q_0, \boldsymbol{\omega}, \hat{\boldsymbol{\vartheta}}, \boldsymbol{\xi}) + \\ \boldsymbol{u}^{\mathrm{T}}\boldsymbol{R}\boldsymbol{u} - \gamma^2\|(\boldsymbol{f}+\boldsymbol{d})\|^2\big]\mathrm{d}\kappa\Big\},\end{aligned} \tag{73}$$

for each $\boldsymbol{\vartheta} \in \mathbf{R}^6$, where

$$\begin{aligned}&l(\boldsymbol{q}, q_0, \boldsymbol{\omega}, \hat{\boldsymbol{\vartheta}}, \boldsymbol{\xi}) = \\ &\quad -4\{c\boldsymbol{q}^{\mathrm{T}}\boldsymbol{\omega} + \boldsymbol{x}^{\mathrm{T}}[(\boldsymbol{\phi}(\boldsymbol{\omega}) + \boldsymbol{\varphi}(\boldsymbol{q}, q_0, \boldsymbol{\omega}))\hat{\boldsymbol{\vartheta}} + \\ &\quad \boldsymbol{r}_1(\boldsymbol{\omega})\boldsymbol{\xi} + \boldsymbol{r}_2(\boldsymbol{q}, q_0, \boldsymbol{\omega})\boldsymbol{\omega}] + \boldsymbol{\xi}^{\mathrm{T}}\boldsymbol{P}(\boldsymbol{A}\boldsymbol{\xi} + \boldsymbol{B}\boldsymbol{\omega})\} + \\ &\quad 4\boldsymbol{x}^{\mathrm{T}}\boldsymbol{R}_1^{-1}\boldsymbol{x} - \frac{4}{\gamma^2}\boldsymbol{x}^{\mathrm{T}}\boldsymbol{x} - \frac{4\tilde{\mu}\dot{\hat{\mu}}}{\hat{\mu}^2}.\end{aligned} \tag{74}$$

Proof From definition of $l(\boldsymbol{q}, q_0, \boldsymbol{\omega}, \hat{\boldsymbol{\vartheta}}, \boldsymbol{\xi})$ in Eq. (74) and the proof of Theorem 3, we have

$$\begin{aligned}&l(\boldsymbol{q}, q_0, \boldsymbol{\omega}, \hat{\boldsymbol{\vartheta}}, \boldsymbol{\xi}) = \\ &\quad -4\Big\{c\boldsymbol{q}^{\mathrm{T}}\boldsymbol{\omega} + \boldsymbol{x}^{\mathrm{T}}\big[\big(\boldsymbol{F}(\boldsymbol{\omega}) + \boldsymbol{G}(\boldsymbol{q}, q_0, \boldsymbol{\omega})\big)\hat{\boldsymbol{\vartheta}} + \\ &\quad \boldsymbol{r}_1(\boldsymbol{\omega})\boldsymbol{\xi} + \boldsymbol{r}_2(\boldsymbol{q}, q_0, \boldsymbol{\omega})\boldsymbol{\omega}\big] + \\ &\quad \boldsymbol{\xi}^{\mathrm{T}}\boldsymbol{P}(\boldsymbol{A}\boldsymbol{\xi} + \boldsymbol{B}\boldsymbol{\omega}) - \boldsymbol{R}_1^{-1}\boldsymbol{x} + \frac{\boldsymbol{x}}{\gamma^2} - \frac{4\tilde{\mu}\dot{\hat{\mu}}}{\hat{\mu}^2}\Big\} \geqslant \\ &\quad 4\Big(\frac{c}{4}\lambda_{\boldsymbol{K}}^{\min}\|\boldsymbol{q}\|^2 + \frac{1}{4}\lambda_{\boldsymbol{K}_1}^{\min}\|\boldsymbol{x}\|^2 + \frac{1}{2}\lambda_{\boldsymbol{\xi}}\|\boldsymbol{\xi}\|^2\Big).\end{aligned} \tag{75}$$

According to the same steps as in Eq. (62) and by completing square

$$\begin{aligned}L_a = &4V_1(0) - \int_0^\infty 2\Big[\frac{\sqrt{2}\boldsymbol{x}}{\gamma} - \frac{\gamma}{\sqrt{2}}(\boldsymbol{f}+\boldsymbol{d})\Big]^{\mathrm{T}} \times \\ &\Big[\frac{\sqrt{2}\boldsymbol{x}}{\gamma} - \frac{\gamma}{\sqrt{2}}(\boldsymbol{f}+\boldsymbol{d})\Big]\mathrm{d}t + \\ &\int_0^\infty (\boldsymbol{u}-\boldsymbol{\alpha}^*)^{\mathrm{T}}\boldsymbol{R}_1(\boldsymbol{u}-\boldsymbol{\alpha}^*)\mathrm{d}t,\end{aligned} \tag{76}$$

the "worst-case" disturbance is given as follows:

$$\boldsymbol{f} + \boldsymbol{d} = \frac{2\boldsymbol{x}}{\gamma^2}.$$

Hence, the minimum of the cost functional L_a is reached only if $\boldsymbol{u} = \boldsymbol{\alpha}^*$, that is, the control law $\boldsymbol{u} = \boldsymbol{\alpha}^*(\boldsymbol{q}, q_0, \boldsymbol{\omega}, \hat{\boldsymbol{\vartheta}}, \tau_{\max})$ given in Eq. (72) with Eqs. (67)—(69) is inverse optimal and minimizes the cost functional Eq. (73). The value function of Eq. (73) is $L_a^* = 4V(0)$.

Remark 9 From $L_a^* = 4V_1(0)$, we obtain

$$\begin{aligned}\int_0^t \big[l(\boldsymbol{q}, q_0, \boldsymbol{\omega}, \hat{\boldsymbol{\vartheta}}, \boldsymbol{\xi}) + \boldsymbol{u}^{\mathrm{T}}\boldsymbol{R}\boldsymbol{u}\big]\mathrm{d}\kappa \leqslant \\ \gamma^2\int_0^t \|\boldsymbol{f}+\boldsymbol{d}\|^2\mathrm{d}\kappa + 4V_1(0),\end{aligned}$$

which implies that the closed-loop system for the feedback control law given in Eq. (72) has $\mathcal{L}_2$ gain less than or equal to γ from the extended disturbance $(\boldsymbol{d}+\boldsymbol{f})$ to the state vector $[\boldsymbol{q}\ \ q_0\ \ \boldsymbol{\omega}\ \ \hat{\boldsymbol{\theta}}\ \ \boldsymbol{\xi}]^{\mathrm{T}}$ and the control input $\boldsymbol{u}$.

Remark 10 The proposed controller is not only robust against the system parametric uncertainties and the external disturbances, but also able to accommodate the actuator faults under control input saturation. Furthermore, it does not require fault detection and isolation mechanism to detect, separate and identify the actuator faults on-line. In addition, if an adaptive parameter update law in Eq. (67) is employed, the information of certain bounds on the effectiveness factors of the actuator is not needed.

Remark 11 In the updating laws, the adaptation laws in Eqs. (67) and (69) can also be modified as

$$\begin{aligned}\dot{\hat{\mu}} &= \mathrm{Proj}_{\hat{\mu}}\Big(\frac{1}{2}\boldsymbol{x}^{\mathrm{T}}\hat{\mu}^3\boldsymbol{\chi}\Big), \\ \dot{\hat{\psi}}_{ij} &= \mathrm{Proj}_{\hat{\psi}}(\boldsymbol{\Gamma}\boldsymbol{S}(\boldsymbol{z})\boldsymbol{x})_{ij}.\end{aligned}$$

3 Numerical Example

Numerical simulations have been conducted for a flexible spacecraft system in Eqs. (2), (4) and (5) with the developed IOAFTC to illustrate and evaluate the effectiveness of the proposed control schemes. For the purpose of comparison, the IOAC and the anti-windup proportional-integral-derivative (AWPID) control method [8,11] are also carried out in the following simulations. The AWPID is designed as

$$\begin{aligned}\boldsymbol{u} = &\boldsymbol{\omega}\times\boldsymbol{J}\boldsymbol{\omega} - K_{\mathrm{d}}\boldsymbol{\omega} - K_{\mathrm{p}}\boldsymbol{q} - \\ &K_{\mathrm{I}}\int\boldsymbol{q}\mathrm{d}t - K_{\mathrm{a}}\int(\boldsymbol{u}_{\mathrm{sat}} - \boldsymbol{u})\mathrm{d}t,\end{aligned} \tag{77}$$

where K_{d}, K_{p}, K_{I} and K_{a} are the designed parameters, and

$$\boldsymbol{u}_{\mathrm{sat}} = \begin{cases} u_{\max}\mathrm{sgn}(\boldsymbol{u}_{\mathrm{sat}}), & |\boldsymbol{u}_{\mathrm{sat}}| > u_{\max} \\ \boldsymbol{u}_{\mathrm{sat}}, & |\boldsymbol{u}_{\mathrm{sat}}| \leqslant u_{\max} \end{cases}.$$

The rest-to-rest maneuver is considered in the simulation. Table 1 gives the numerical simulation parameters. These parameters are used for all cases of the simulation. In the simulation analysis, only the first three elastic modes are considered in the controller design, due to the possible spillover effects. Two cases of actuator are considered to demonstrate the superior performance of the addressed fault-tolerant controller, i.e., all actuators are healthy and time-varying loss of actuator effectiveness and time-varying additive faults, respectively.

Table 1 Simulation parameters

Parameter	Definiton
Mass moment of inertia tensor	$\boldsymbol{J}_0 = \begin{bmatrix} 350 & 3 & 4 \\ 3 & 280 & 10 \\ 4 & 10 & 190 \end{bmatrix}$ kg/m^2
Natural frequency	$\omega_{\mathrm{n}1} = 0.768\,1$ rad/s, $\omega_{\mathrm{n}2} = 1.103\,8$ rad/s, $\omega_{\mathrm{n}3} = 1.873\,3$ rad/s, $\omega_{\mathrm{n}4} = 2.549\,6$ rad/s
Damping ration	$\xi_1 = 0.005\,6$, $\xi_2 = 0.008\,6$, $\xi_3 = 0.013$, $\xi_4 = 0.025$
Coupling matrix	$\boldsymbol{\sigma} = \begin{bmatrix} 6.456\,37 & 1.278\,14 & 2.156\,29 \\ -1.256\,19 & 0.917\,56 & -1.672\,64 \\ 1.116\,87 & 2.489\,01 & -0.836\,74 \\ 1.236\,37 & -2.658\,1 & -1.125\,03 \end{bmatrix}$
Initial conditions	$\boldsymbol{q}(0) = [-0.2 \quad 0.7 \quad -0.35]^{\mathrm{T}}$, $\boldsymbol{\omega}(0) = [0 \quad 0 \quad 0]^{\mathrm{T}}$, $\boldsymbol{\eta}_i(0) = \dot{\boldsymbol{\eta}}_i(0) = \mathbf{0}$ $(i = 1, 2, 3, 4)$, $\hat{\boldsymbol{\vartheta}}(0) = [340 \quad 290 \quad 175 \quad 1 \quad 2 \quad 10]$, $\hat{\mu}(0) = 1$
External disturbance	$\boldsymbol{d}(t) = (\Vert\boldsymbol{\omega}\Vert^2 + 0.15)[\cos(0.1t) \quad \sin(0.5t) \quad \sin(0.35t)]$
Control parameters (IOAC, IOAFTC and AWPID)	$c = 1\,200$, $\boldsymbol{K} = 0.4\boldsymbol{I}_3$, $\boldsymbol{K}_1 = 700\boldsymbol{I}_3$, $\boldsymbol{\Pi} = 200\boldsymbol{I}_6$, $\gamma = 2$, $\varepsilon_{\mathrm{N}} = 0.005$, $K_{\mathrm{d}} = 100$, $K_{\mathrm{p}} = 100$, $K_{\mathrm{I}} = 1$, $K_{\mathrm{a}} = 0.5$
Maximum allowable torque input	$u_{\max} = 5$ N·m
RPF NN	$m = 20$, $d_i (i = 1, 2, \cdots, 20)$ evenly spaced in $[-\pi/5, \pi/5] \times [-\pi/5, \pi/5] \times [-\pi/5, \pi/5]$, $a = \pi/20$

3.1 Healthy Actuators

In this case, all actuators are considered to be healthy, i.e., $\boldsymbol{f} = \mathbf{0}_{3\times1}$ and $\boldsymbol{\delta} = \boldsymbol{I}_3$. The numerical results of the simulations obtained by IOAC, IOAFTC and AWPID are presented in Figs. 1—4. The quaternion and angular velocity responses of the attitude system are shown in Figs. 1 and 2, respectively. One can observe that, for both IOAC and IOAFTC, high control precision of the attitude and angular velocity is obtained within 20 s even in the presence of system parametric uncertainties, external disturbances and under control input saturation, while for AWPID, it experiences more than 50 s to stabilize the attitude, which is longer than that of IOAC and IOAFC. In addition, it can be found that the pointing precision of IOAC and

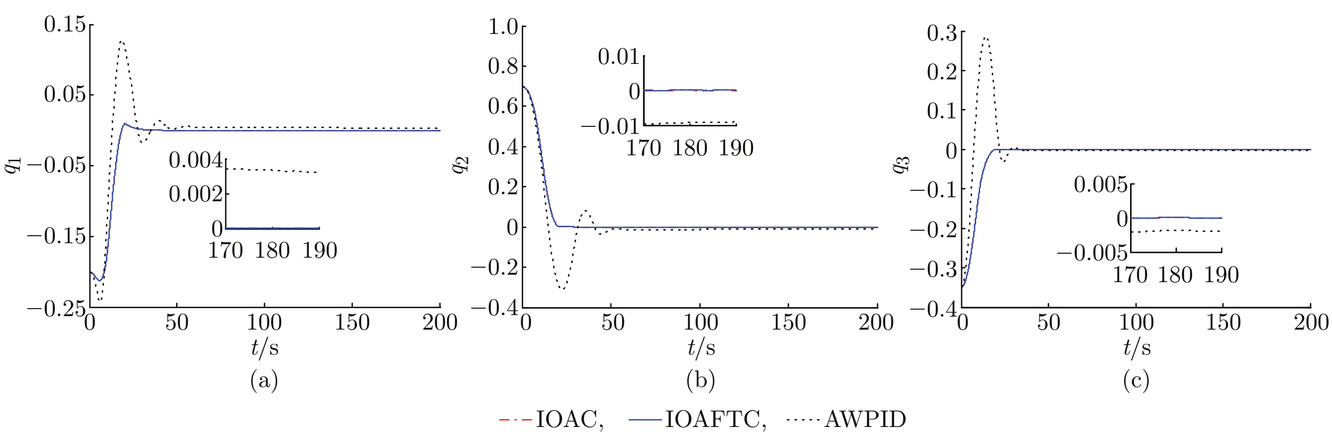

Fig. 1 Time responses of quaternion with healthy actuators

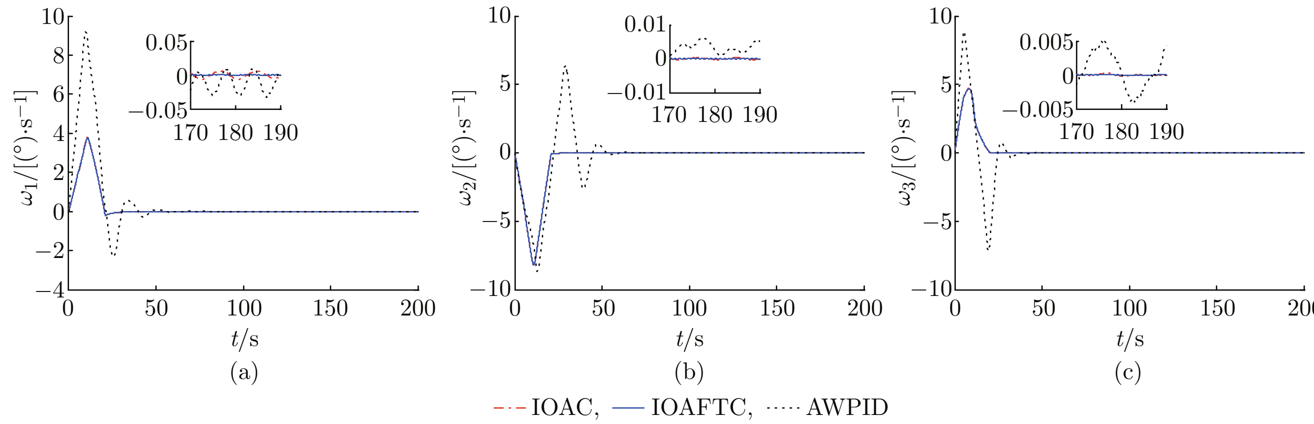

Fig. 2 Time responses of angular velocity with healthy actuators

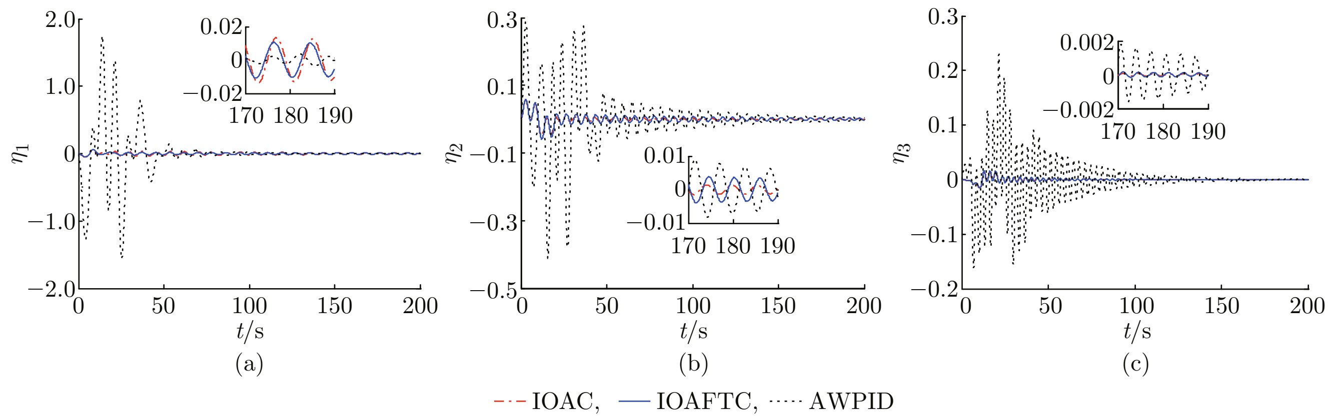

Fig. 3 Time responses of flexible vibration with healthy actuators

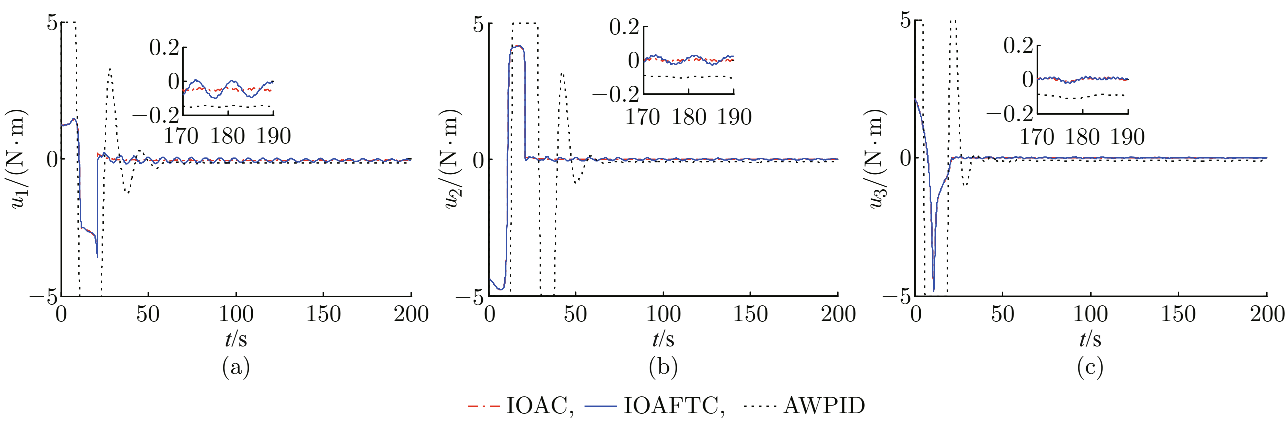

Fig. 4 Time responses of thruster outputs with healthy actuators

IOAFTC is higher than that of AWPID. The responses of the modal displacements η_1, η_2 and η_3 are presented in Fig. 3, in which a low vibration level for the proposed IOAC and IOAFTC is illustrated and there are almost no oscillations after 20 s. This illustrates that the designed controllers are capable of suppressing the system vibration while controlling the attitude of the spacecraft with the healthy actuators. While for AWPID, there exist severe oscillations, and the eventually settling time is more than 150 s. The applied control torques on the flexible spacecraft are shown in Fig. 4. It can be observed that more output torques are needed for AWPID in comparison with IOAC and IOAFC.

3.2 Actuator Fault

In this case, we consider the conditions that both the partial loss of actuator effectiveness and the additive faults occur. Each actuator undergoes a serious partial loss of effectiveness and an additive fault at $t \geqslant 10\,\mathrm{s}$. The actuator effectiveness matrix $\boldsymbol{\delta} = \mathrm{diag}\{\delta_{11}, \delta_{22}, \delta_{33}\}$ and the additive fault vector $\boldsymbol{f}$ are respectively given by

$$\delta_{ii}(t) = \begin{cases} 1, & t < 10\,\mathrm{s} \\ 0.35 + 0.2\sin(2\pi t), & t \geqslant 10\,\mathrm{s} \end{cases},$$

$$f_i(t) = \begin{cases} 1, & t < 10\,\mathrm{s} \\ 0.35 + 0.05\sin(2\pi t), & t \geqslant 10\,\mathrm{s} \end{cases}.$$

Figures 5—8 show the simulated results obtained by IOAC, IOAFTC and AWPID, respectively. It can be seen that for IOAFTC, a fairly good control performance is achieved within 20 s and no significant amount of vibration occurs even under the severe thruster faults after 10 s. For IOAC, it can be observed that when the actuator experiences serious partial loss of effectiveness and additive faults after 10 s, it experiences more than 100 s to stabilize the attitude and severe oscillations are excited again by maneuvering. While for AWPID, it is found that when the actuator faults occur after 10 s, the attitude pointing accuracy becomes very low and

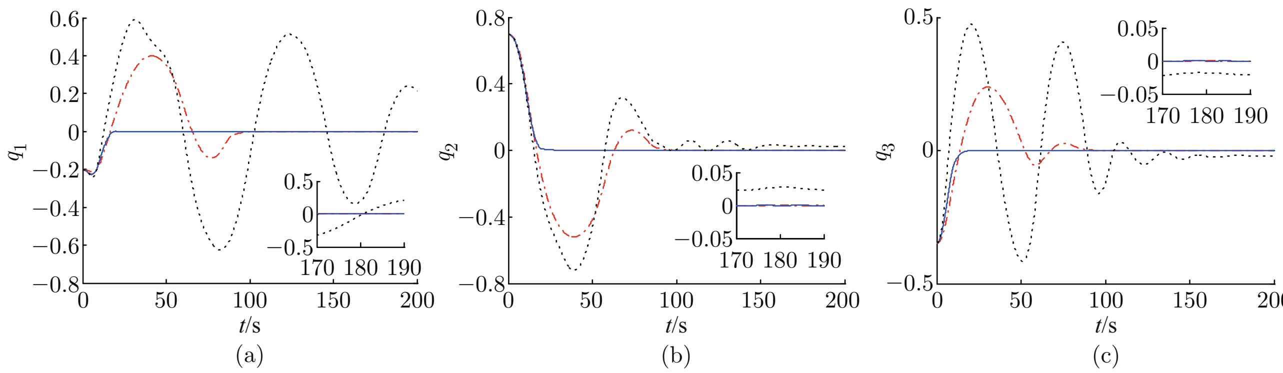

-·-IOAC, —IOAFTC, ·····AWPID

Fig. 5 Time responses of quaternion with fault acturators

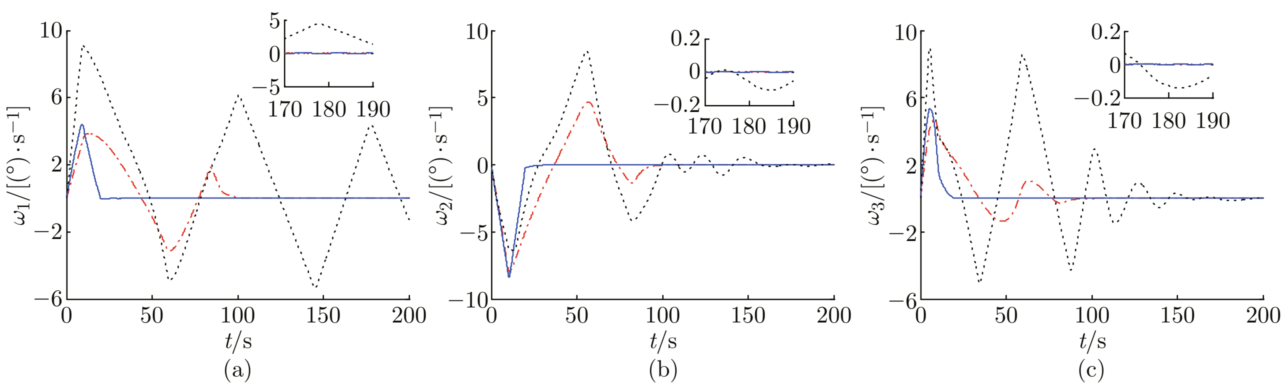

-·-IOAC, —IOAFTC, ·····AWPID

Fig. 6 Time responses of angular velocity with fault actuators

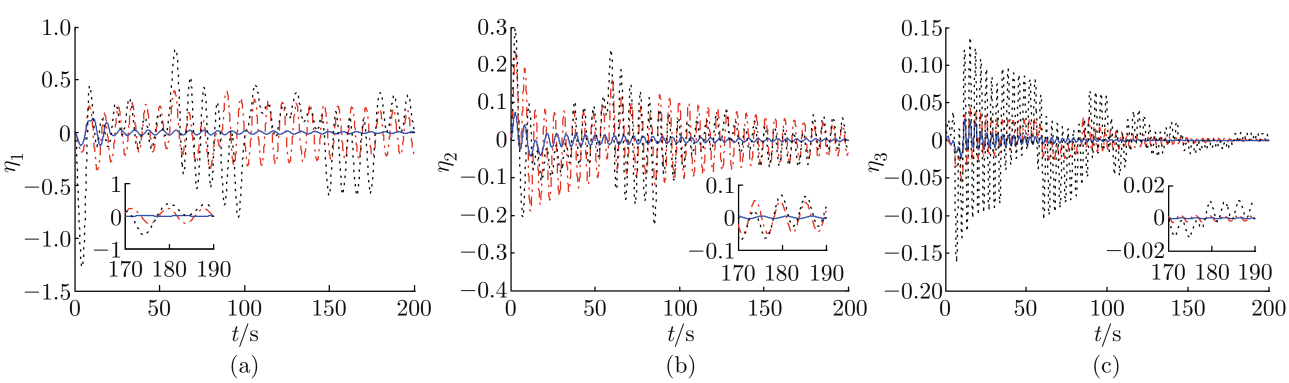

-·-IOAC, —IOAFTC, ·····AWPID

Fig. 7 Time responses of flexible vibration with fault actuators

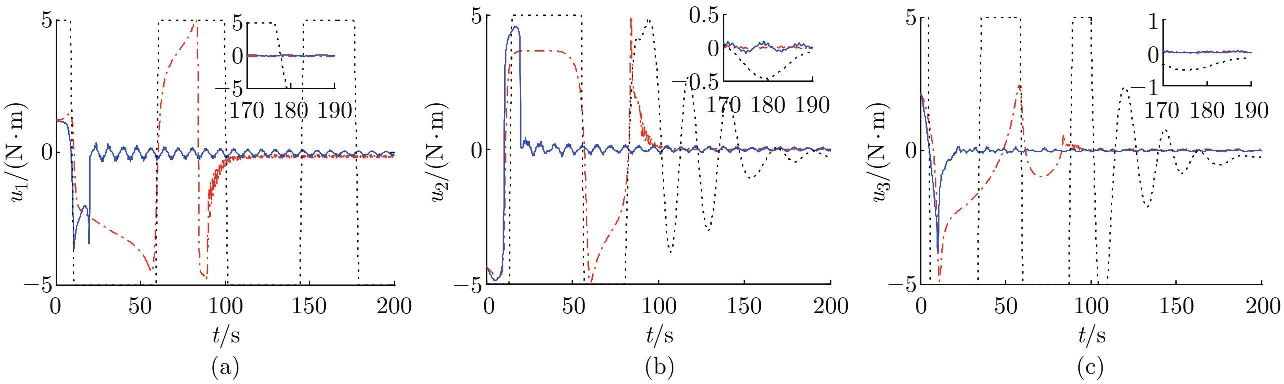

Fig. 8 Time responses of thruster outputs with fault actuators

the severe oscillations are also excited again by maneuvering. Moreover, it is unable to maintain stability and therefore cannot satisfy the requirement of the mission. The reason of this behaviour is that once the actuators undergo partial loss of effectiveness especially the serious case, the value of control input is not big enough to compensate the fault. From the simulation results, we can conclude that the IOAFTC can significantly improve the control performance over those of the IOAC and AWPID subjected to the actuator faults, input saturation, inertia matrix uncertainty and external disturbances. Further, extensive simulations are also done using different control parameters.

4 Conclusion

This paper presents a fault-tolerant attitude control algorithm for the flexible spacecraft in the presence of actuator fault, control input saturation, parametric uncertainty and external disturbances. The control algorithm is based on an adaptive control Lyapunov function and an inverse optimal methodology, which can guarantee robustness and stabilization and achieve H_∞ optimality with respect to a family of cost functionals. The proposed adaptive fault-tolerant controller doesn't require the process of fault identification, detection and isolation, and even the information of certain bounds on the effectiveness factors of the actuator is not needed. The control design is assessed and compared to other methods through numerical simulations. The results show that the proposed fault-tolerant attitude controller is able to accommodate the actuator fault and achieve high precision pointing while the conventional methods fail to attain the control objective.

References

[1] JIN J H, KO S H, RYOO C K. Fault tolerant control for satellites with four reaction wheels [J]. *Control Engineering Practice*, 2008, **16**(10): 1250-1258.

[2] HU Q L. Robust adaptive sliding-mode fault-tolerant control with $\mathcal{L}_2$-gain performance for flexible spacecraft using redundant reaction wheels [J]. *IET Control Theory and Applications*, 2009, **4**(6): 1055-1070.

[3] MENG Q, ZHANG T, SONG J Y. Modified model-based fault-tolerant time-varying attitude tracking control of uncertain flexible satellites [J]. *Proceedings of the Institution of Mechanical Engineers, Part G: Journal of Aerospace Engineering*, 2013, **227**(11): 1827-1841.

[4] HU Q L, XIAO B, FRISWELL M I. Robust fault-tolerant control for spacecraft attitude stabilization subject to input saturation [J]. *IET Control Theory and Application*, 2011, **5**(2): 271-282.

[5] LEE H, KIM Y. Fault-tolerant control scheme for satellite attitude control system [J]. *IET Control Theory and Application*, 2010, **4**(8): 1436-1450.

[6] XIAO B, HU Q L. Fault-tolerant attitude control for flexible spacecraft without angular velocity magnitude measurement [J]. *Journal of Guidance, Control, and Dynamics*, 2011, **34**(5): 1556-1561.

[7] BOŠKOVIĆ J D, LI S M, MEHRA R K. Robust adaptive variable structure control of spacecraft under control input saturation [J]. *Journal of Guidance, Control, and Dynamics*, 2001, **24**(1): 14-22.

[8] BANG H, TAHK M J, CHOI H D. Large angle attitude control of spacecraft with actuator saturation [J]. *Control Engineering Practice*, 2003, **11**: 989-997.

[9] CAI W C, LIAO X H, SONG Y D. Indirect robust adaptive fault-tolerant control for attitude tracking of spacecraft [J]. *Journal of Guidance, Control, and Dynamics*, 2008, **31**(5): 1456-1463.

[10] ZOU A M, KUMAR K D. Adaptive fuzzy fault-tolerant attitude control of spacecraft [J]. *Control Engineering Practice*, 2011, **19**: 10-21.

[11] HU Q L, XIAO B. Fault-tolerant sliding mode attitude control for flexible spacecraft under loss of actuator effectiveness [J]. *Nonlinear Dynamics*, 2011, **64**: 13-23.

[12] HORRI N M, PALMER P, ROBERTS M. Design and validation of inverse optimization software for the attitude control of microsatellites [J]. *Acta Astronautica*, 2011, **69**: 997-1006.

[13] Xin M, Pan H. Indirect robust control of spacecraft via optimal control solution [J] *IEEE Transactions on Aerospace and Electronic Systems*, 2012, **48**(2): 1798-1809.

[14] Nayeri M R D, Alasty A, Daneshjou K. Neural optimal control of flexible spacecraft slew maneuver [J]. *Acta Astronautica*, 2004, **55**: 817-827.

[15] Zheng J H, Banks H G, Alleyne H. Optimal attitude control for three-axis stabilized flexible spacecraft [J]. *Acta Astronautica*, 2005, **56**: 519-528.

[16] Park Y. Robust and optimal attitude stabilization of spacecraft with external disturbances [J]. *Aerospace Science and Technology*, 2005, **9**: 253-259.

[17] Kang W. Nonlinear H_∞ control and its application to rigid spacecraft [J]. *IEEE Transactions on Automatic Control*, 1995, **40**(7): 1281-1285.

[18] Zheng Q, Wu F. Nonlinear H_∞ control designs with axisymmetric spacecraft control [J]. *Journal of Guidance, Control, and Dynamics*, 2009, **32**(3): 850-859.

[19] Liu C S, Jiang B. H_∞ fault-tolerant control for time-varied actuator fault of nonlinear system [J]. *International Journal of Systems Science*, 2014, **45**(12): 2447-2457.

[20] Li Z, Hu Y, Liu Y, et al. Adaptive inverse control of non-linear systems with unknown complex hysteretic non-linearities [J]. *IET Control Theory and Applications*, 2012, **6**(1): 1-7.

[21] Krstić M, Li Z H. Inverse optimal design of Input-to-State stabilizing nonlinear controllers [J]. *IEEE Transactions on Automatic Control*, 1998, **43**(3): 336-350.

[22] Cai X S, Han Z Z. Inverse optimal control of nonlinear systems with structural uncertainty [J]. *IET control Theory and Applications*, 2005, **152**(1): 79-83.

[23] Bharadwaj S, Qsipchuk M, Mease K D, et al. Geometry and inverse optimality in global attitude stabilization [J]. *Journal of Guidance, Control, and Dynamics*, 1998, **21**(6): 930-939.

[24] Krstić M, Tsiotras P. Inverse optimal stabilization of a rigid spacecraft [J]. *IEEE Transactions on Automatic Control*, 1999, **44**(5): 1042-1049.

[25] Luo W C, Chu Y C, Ling K V. H_∞ inverse optimal attitude-tracking control of rigid spacecraft [J]. *Journal of Guidance, Control, and Dynamics*, 2005, **28**(3): 481-493.

[26] Luo W C, Chu Y C, Ling K V. Inverse optimal adaptive control for attitude tracking of spacecraft [J]. *IEEE Transactions on Automatic Control*, 2005, **50**(11): 1639-1654.

[27] Krstić M, Kanellakopoulos I, Kokotovic P V. Nonlinear and adaptive control design [M]. New York: Wiley, 1995.

[28] Ahmed J, Coppola V T, Bernstein D S. Adaptive asymptotic tracking of spacecraft attitude notion with inertia matrix identification [J]. *Journal of Guidance, Control, and Dynamics*, 1998, **21**(5), 684-691.

[29] Chen Z Y, Huang J. Attitude tracking and disturbance rejection of rigid spacecraft by adaptive control [J]. *IEEE Transaction on Automatic Control*, 2009, **54**(3): 600-605.

[30] Gao W Z, Selmic R R. Neural network control of a class of nonlinear systems with actuator saturation [J]. *IEEE Transactions on Neural Networks*, 2006, **17**(1): 147-156.

[31] Hu Q L, Xiao B. Intelligent proportional-derivative control for flexible spacecraft attitude stabilization with unknown input saturation [J]. *Aerospace Science and Technology*, 2012, **23**: 63-74.

[32] Funahashi K I. On the approximate realization of continuous mappings by neural networks [J]. *Neural Networks*, 1989, **2**(3): 183-192.

[33] Khalil H K. Nonlinear systems [M]. Upper Saddle River, NJ: Prentice-Hall, 1996.

[34] Yao B, Tomizuka M. Smooth robust adaptive sliding mode control of robot manipulators with guaranteed transient performance [J]. *Journal of Dynamics systems, Measurement and Control*, 1996, **118**(4): 764-775.